

# Rhodium Complexes with Pincer Diphosphite Ligands. Unusual Olefin in-Plane Coordination in Square-Planar Compounds<sup>†</sup>

Miguel Rubio,<sup>‡</sup> Andrés Suárez,<sup>‡</sup> Diego del Río,<sup>‡,§</sup> Agustín Galindo,<sup>\*,⊥</sup> Eleuterio Álvarez,<sup>‡</sup> and Antonio Pizzano<sup>\*,‡</sup>

*Instituto de Investigaciones Químicas, Consejo Superior de Investigaciones Científicas, and Universidad de Sevilla, Avda Américo Vespucio no. 49, Isla de la Cartuja, 41092 Sevilla, Spain, and Departamento de Química Inorgánica, Universidad de Sevilla, Aptdo 1203, 41071 Sevilla, Spain*

Received August 26, 2008

A family of rhodium complexes bearing pincer diphosphite (PCP) and neutral L (L = PPh<sub>3</sub>, CO, CNXy, C<sub>2</sub>H<sub>4</sub>) ligands has been prepared and characterized. Reactions between Rh(Cl)(PPh<sub>3</sub>)<sub>3</sub> and the diphosphites **2** lead to the chloro hydrides Rh(H)(Cl)(PCP)(PPh<sub>3</sub>) (**4**), which can be deprotonated to yield the complexes Rh(PCP)(PPh<sub>3</sub>) (**5**). In the latter, the PPh<sub>3</sub> ligand is labile and can be exchanged by CO, CNXy, and C<sub>2</sub>H<sub>4</sub> to give derivatives **6–8**. Most noteworthy is the fact that ethylene complexes **8a,b** show a remarkable in-plane (*ip*) conformation in the solid state. Solution NMR studies for these complexes show fast olefin rotation in all the temperature ranges, while solution and solid-state <sup>13</sup>C{<sup>1</sup>H} NMR experiments give practically superimposable spectra, also indicating the prevalence of the *ip* conformer in solution. Complementary detailed DFT calculations performed with models of compounds **8** indicate that the olefin conformational preference is due to a dual combination of steric effects arising from the reduction of the P–Rh–P angle from 180°, caused by pincer ligand chelation and by the nature of the phosphite substituents, which in the case of *t*-Bu groups perfectly outline a cavity for an *ip* coordination of the olefin.

## Introduction

The orientation of a coordinated olefin is an aspect of fundamental interest in organometallic chemistry, and it is of great importance in relation to the stereochemistry of reactions involving alkene transformation.<sup>1</sup> The preferred conformation for a metal-bonded olefin is explained by the Chatt–Dewar–Duncanson model<sup>2,3</sup> and, more specifically, by the existence of a back-bonding component from a metal-centered orbital to the π\* olefin orbital. As a result, the orientation of the olefin depends on the geometry of the complex.<sup>4</sup> For the important class of square-planar compounds, in-plane (*ip*) and upright (*u*) olefin orientations are electronically of similar energy. However, steric effects between the olefin and cis coligands L<sub>c</sub> are lower in the

*u* orientation.<sup>5</sup> This steric preference is marked indeed, and a perusal of the structures of square-planar olefin complexes described in the literature indicates that the *u* conformation has almost exclusively been observed. However, two cases can be considered exceptions to this general behavior. The first regards Pt and Pd cationic complexes of the formulation [M(alkene)-(allyl)(phosphine)]<sup>+</sup> (**A**). These complexes display different olefin orientations depending on the nature of this ligand, including several cases of *ip* conformation. Due to the small bite angle of the allyl ligand, the definition of their structure is not unambiguous and they have either been assigned as square-planar<sup>6</sup> or planar-trigonal complexes,<sup>7</sup> which in turn have a clear preference for an in-plane conformation.<sup>4</sup> The second pertinent case is constituted by the complexes of the methylene cycloheptene diolefin (**B**), which due to the perpendicularity between the two olefinic bonds forces an *ip* conformation of one of the alkene fragments.<sup>8</sup> In view of these precedents, there is not a clear-cut case of a square-planar complex in which, the two conformations being accessible, *ip* is preferred.



\* To whom correspondence should be addressed. E-mail: galindo@us.es (A.G.); pizzano@iiq.csic.es (A.P.).

<sup>†</sup> This article is dedicated to Prof. Ernesto Carmona on the occasion of his 60th birthday.

<sup>‡</sup> Instituto de Investigaciones Químicas.

<sup>§</sup> Present address: SRI International, 333 Ravenswood Avenue, Menlo Park, CA 94065.

<sup>⊥</sup> Universidad de Sevilla.

(1) For some representative studies of olefin reactivity considering orientation, see: (a) Musaev, D. G.; Svensson, M.; Morokuma, K.; Strömberg, S.; Zetterberg, K.; Siegbahn, P. E. M. *Organometallics* **1997**, *16*, 1933. (b) Gridnev, I. D.; Yasutake, M.; Higashi, N.; Imamoto, T. *J. Am. Chem. Soc.* **2001**, *123*, 5268. (c) Carbó, J. J.; Lledós, A.; Vogt, D.; Bo, C. *Chem. Eur. J.* **2006**, *12*, 1457. (d) Adlhart, C.; Chen, P. *J. Am. Chem. Soc.* **2004**, *126*, 3496. (e) Sakaki, S.; Mizoe, N.; Sugimoto, M.; Musashi, Y. *Coord. Chem. Rev.* **1999**, *190*, 933.

(2) (a) Chatt, J.; Duncanson, L. A. *J. Chem. Soc.* **1953**, 2939. (b) Dewar, M. J. S. *Bull. Chem. Soc. Chim. Fr.* **1951**, C71.

(3) Recent studies of the metal–olefin bond: (a) Frenking, G.; Fröhlich, N. *Chem. Rev.* **2000**, *100*, 717. (b) Price, D. W.; Drew, M. G. B.; Hii, K. K.; Brown, J. M. *Chem. Eur. J.* **2000**, *6*, 4587. (c) Tsepis, A. C. *Organometallics* **2008**, *27*, 3701.

(4) Albright, T. A.; Hoffmann, R.; Thibault, J. C.; Thorn, D. L. *J. Am. Chem. Soc.* **1979**, *101*, 3801.

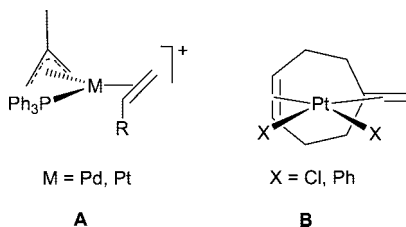
(5) (a) Hay, P. J. *J. Am. Chem. Soc.* **1981**, *103*, 1390. (b) Ziegler, T.; Rauk, A. *Inorg. Chem.* **1979**, *18*, 1558. (c) Senn, H. M.; Blöchl, P. E.; Togni, A. *J. Am. Chem. Soc.* **2000**, *122*, 4098.

(6) (a) Miki, K.; Kai, Y.; Kasai, N.; Kurosawa, H. *J. Am. Chem. Soc.* **1983**, *105*, 2482. (b) Kurosawa, H.; Miki, K.; Kasai, N.; Ikeda, I. *Organometallics* **1991**, *10*, 1607.

(7) Musco, A.; Pontellini, R.; Grassi, M.; Sironi, A.; Meille, S. V.; Rüegger, H.; Ammann, C.; Pregosin, P. S. *Organometallics* **1988**, *7*, 2130.

(8) Rakowsky, M. H.; Woolcock, J. C.; Wright, L. L.; Green, D. B.; Rettig, M. F.; Wing, R. M. *Organometallics* **1987**, *6*, 1211.

On the other hand, pincer ligands are also of great interest, due to their marked ability to stabilize transition-metal complexes.<sup>9</sup> Among them, those possessing two donor phosphine fragments constitute a prominent group. Otherwise, pincer accepting ligands have largely remained unexplored and only recently have attracted the attention of researchers. Thus, new ligands based on fluorophosphines,<sup>10</sup> *N*-pyrrolyl phosphines,<sup>11</sup> and phosphites<sup>12</sup> have recently been described.

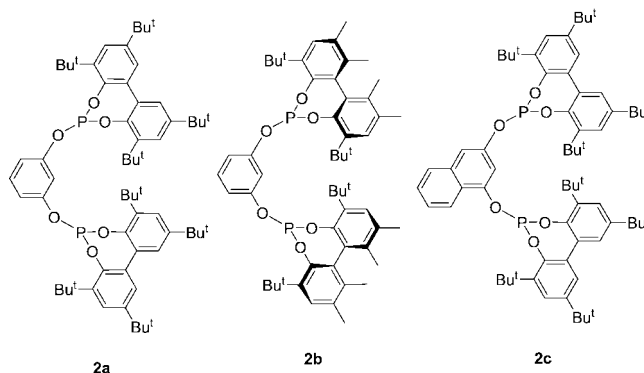
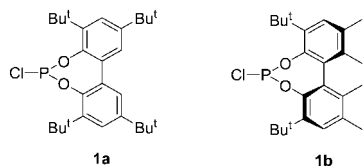
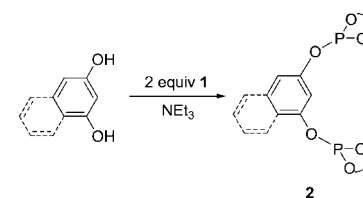


In this contribution we describe a group of novel diphosphites and their incorporation into rhodium complexes, these being the first examples of rhodium–pincer diphosphite complexes. These pincer ligands outline a spatial distribution of steric hindrance which differs from that exhibited by a fragment  $ML_3$ , which makes possible a preferred ethylene in-plane coordination in square-planar complexes. These olefinic derivatives have been studied in detail by both structural and theoretical methods. The results have been completed with the synthesis and characterization of isocyanide and carbonyl derivatives which provide information about the acceptor character of these pincer ligands. Part of this work has been communicated in a preliminary form.<sup>13</sup>

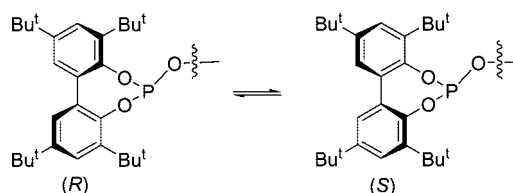
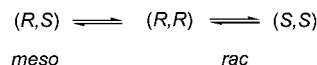
## Results and Discussion

**Ligand Synthesis.** Diphosphites **2** have been prepared by a condensation between resorcinol or 1,3-naphthalenediol and the appropriate chlorophosphite **1** in the presence of a base in good yields (Scheme 1). NMR spectroscopic characterization reflects the differences in symmetry and conformational flexibility among compounds **2**. Thus, **2a** exhibits in the  $^{31}P\{^1H\}$  NMR spectrum one singlet in the typical region of phosphites, while in the  $^1H$  and  $^{13}C\{^1H\}$  experiments we observe the equivalence of the halves of each biphenyl, as well as the other phosphite fragments. This behavior can be explained by a fast interconversion between *rac* and *meso* isomers (Scheme 2). Otherwise, the presence of the naphthyl backbone in compound **2c** renders two phosphite fragments inequivalent, as shown by two singlets in the  $^{31}P\{^1H\}$  NMR spectrum. Moreover, rapid isomerization makes two aryl fragments of each biaryl equivalent in the  $^{13}C\{^1H\}$  and  $^1H$  NMR experiments. Finally, the atropisomeric diphosphite **2b** exhibits spectra which account for its  $C_2$  symmetry. Therefore, the two  $^{31}P$  nuclei are equivalent, but two types of biphenyl aryl rings appear in the  $^1H$  and  $^{13}C\{^1H\}$  NMR spectra, those of each inequivalent biphenyl.

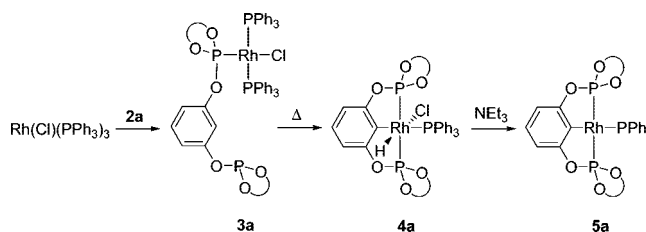
Scheme 1



Scheme 2



Scheme 3



**Preparation and Characterization of  $PPh_3$  Derivatives.** In order to incorporate diphosphites **2** as pincer ligands in Rh complexes, the reaction between **2a** and  $RhCl(PPh_3)_3$  has been studied (Scheme 3). Interaction at room temperature, monitored by  $^{31}P\{^1H\}$  NMR, indicates the formation of the species **3a** characterized by three signals: a singlet at  $\delta$  139.9 indicative of an uncoordinated phosphite, a doublet of doublets of doublets ( $\delta$  128.4,  $J_{RhP} = 336$  Hz,  $J_{PP} = 47, 41$  Hz) in the coordinated phosphite region, and finally, an AB system doubly split by phosphorus and rhodium couplings centered at 36.0 ppm ( $J_{AB} = 356$  Hz,  $J_{RhP} = 138$  Hz), due to two inequivalent  $PPh_3$  groups. Subsequent heating of the solution produces the activation of the central C–H bond and the displacement of another molecule of  $PPh_3$ , thus generating chloro hydride **4a**, which incorporates

(9) van der Boom, M. E.; Milstein, D. *Chem. Rev.* **2003**, *103*, 1759.

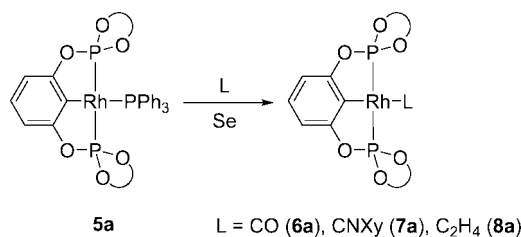
(10) Chase, P. A.; Gagliardo, M.; Lutz, M.; Spek, A. L.; van Klink, G. P. M.; van Koten, G. *Organometallics* **2005**, *24*, 2016.

(11) Kossoy, E.; Iron, M. A.; Rybtchinski, B.; Ben-David, Y.; Shimon, L. J. W.; Konstantinovskii, L.; Martin, J. M. L.; Milstein, D. *Chem. Eur. J.* **2005**, *11*, 2319.

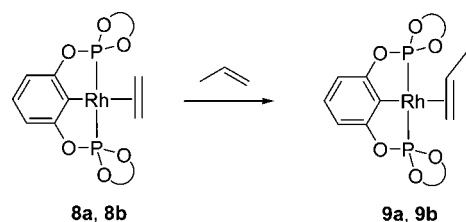
(12) (a) Barber, R. A.; Bedford, R. B.; Betham, M.; Blake, M. E.; Coles, S. J.; Haddow, M. F.; Hursthouse, M. B.; Orpen, A. G.; Pilarski, L. T.; Pringle, P. G.; Wingard, R. L. *Chem. Commun.* **2006**, 3880. (b) Miyazaki, F.; Yamaguchi, K.; Shibasaki, M. *Tetrahedron Lett.* **1999**, *40*, 7379.

(13) Rubio, M.; Suárez, A.; del Río, D.; Galindo, A.; Álvarez, E.; Pizzano, A. *Dalton Trans.* **2007**, 407.

Scheme 4



Scheme 5



a pincer diphosphite ligand (PCP<sup>a</sup>).<sup>14</sup> The presence of a hydride ligand in the latter complex is characterized in the IR spectrum by a band at 2112 cm<sup>-1</sup> due to  $\nu(\text{Rh}-\text{H})$  and in the <sup>1</sup>H NMR experiment by a doublet of quartets at  $\delta$  -14.8. In the latter, coincident couplings of 12 Hz are observed with the three <sup>31</sup>P and the <sup>103</sup>Rh nuclei. These values are in good accord with the hydride coordinated in a *cis* position with respect to the three phosphorus ligands. The <sup>31</sup>P{<sup>1</sup>H} NMR spectrum is characterized by a doublet of doublets for the two diphosphite <sup>31</sup>P nuclei at 149.9 ppm ( $J_{\text{RhP}} = 178$  Hz,  $J_{\text{PP}} = 35$  Hz) and a doublet of triplets at 13.7 ppm ( $J_{\text{RhP}} = 87$  Hz) for a coordinated PPh<sub>3</sub>. The value of  $J_{\text{RhP}}$  is similar to those found in compounds with chloride and hydride ligands occupying mutually trans positions.<sup>15,16</sup> This arrangement has been definitively ascertained by an X-ray diffraction study (see the Supporting Information).

Heating the solution of compound **3a** also produces a small amount of complex **5a**, which results from the loss of HCl from chloro hydride **4a**. Subsequent addition of an excess of NEt<sub>3</sub> facilitates this step and results in the isolation of **5a** in good yield. NMR spectra for complex **5a** show the expected signals for the pincer and PPh<sub>3</sub> ligands. Interestingly, the equivalence of the four aryl biphenyls is observed in the <sup>1</sup>H and <sup>13</sup>C{<sup>1</sup>H} spectra at room temperature, indicative of a fast interconversion between *rac* and *meso* conformers. Derivatives Rh(PCP<sup>b</sup>)(PPh<sub>3</sub>) (**5b**) and Rh(PCP<sup>c</sup>)(PPh<sub>3</sub>) (**5c**) have been prepared by following the procedure described for **5a**.

**Synthesis and Characterization of the Complexes Rh(PCP)L (L = CO, CNXy, H<sub>2</sub>C=CH<sub>2</sub>, H<sub>3</sub>CCH=CH<sub>2</sub>).** The PPh<sub>3</sub> ligand in compound **5a** is labile and can be replaced by other L ligands. Thus, exposing **5a** to an atmosphere of CO readily produces compound **6a** (Scheme 4). However, the released phosphine interferes in the purification of the carbonyl product, as solvent evaporation during the workup procedure is accompanied by regeneration of the phosphine derivative **4a**. Addition of Se to the reaction mixture quenches the phosphine as P(Se)Ph<sub>3</sub>, which can be easily removed from the mixture.<sup>17</sup> This procedure has also been used in the synthesis of the isocyanide compound **7a**. NMR characterization of these complexes shows signals for the pincer and the L ligands. Most meaningful of the presence of the latter is a low-field doublet of triplets in the <sup>13</sup>C{<sup>1</sup>H} spectrum for Rh-CO ( $J_{\text{RhC}} = 58$  Hz,  $J_{\text{PC}} = 16$  Hz) and Rh-CNXY ( $J_{\text{RhP}} = 56$  Hz,  $J_{\text{PP}} = 18$  Hz). As in the case of the phosphine derivative **5a**, these complexes also show fluxional behavior in solution resulting from a fast isomerization of phosphite fragments.

(14) In the article the pincer ligands generated by deprotonation of diphosphites **2a-c** will be denoted PCP<sup>a</sup>, PCP<sup>b</sup>, and PCP<sup>c</sup>, respectively, while PCP will be used to generally refer to them.

(15) The magnitude of  $J_{\text{PRh}}$  depends markedly on the ligand situated in a position trans respect to the P ligand: Naaktgeboren, A. J.; Nolte, R. J. M.; Drenth, W. *J. Am. Chem. Soc.* **1980**, *102*, 3350.

(16) Liou, S.-Y.; Gozin, M.; Milstein, D. *J. Am. Chem. Soc.* **1995**, *117*, 9774.

(17) For alternative quenchers for this reaction, see: (a) Gorla, F.; Venanzi, L. M.; Albinati, A. *Organometallics* **1994**, *13*, 43. (b) Reference 11.

An interesting feature of these pincer-type diphosphite ligands is its acceptor character due to the  $\pi$ -acidity of the phosphite groups. This characteristic has been investigated by IR spectroscopy on complexes **6a** and **7a**, as the magnitudes of  $\nu(\text{CO})$  and  $\nu(\text{CN})$  have diagnostic value. Thus, the carbonyl gives the corresponding band at 2017 cm<sup>-1</sup>,<sup>18</sup> considerably shifted to higher energy from that of analogous derivatives of diphosphinite (1962 cm<sup>-1</sup>)<sup>19</sup> or aryldiphosphine (1955 cm<sup>-1</sup>) pincer complexes.<sup>20</sup> The isonitrile derivative reinforces this observation,<sup>21</sup> as the band for  $\nu(\text{CN})$  appears at 2099 cm<sup>-1</sup>, only 15 cm<sup>-1</sup> lower than in the free isonitrile and considerably higher than the value of 2048 cm<sup>-1</sup> observed in *trans*-RhCl(CNXy)(P-Pr<sup>i</sup>)<sub>2</sub>.<sup>22</sup>

The ethylene complex Rh(PCP<sup>a</sup>)(C<sub>2</sub>H<sub>4</sub>) (**8a**) has also been prepared according to Scheme 4, but this transformation is slow compared with those of CO or CNXy and requires heating of the reaction mixture to 40 °C for 4 days under 4 atm of ethylene to get a good yield. Under similar conditions the derivatives Rh(PCP<sup>b</sup>)(C<sub>2</sub>H<sub>4</sub>) (**8b**) and Rh(PCP<sup>c</sup>)(C<sub>2</sub>H<sub>4</sub>) (**8c**) have also been obtained.<sup>23</sup> Analytical and spectroscopical data for complexes **8** are in good accord with the proposed formulation. Thus, the NMR experiments show, in addition to the signals of the PCP ligand, the pertinent resonances for a coordinated ethylene. For instance, in the <sup>13</sup>C{<sup>1</sup>H} NMR spectrum a relatively broad signal at ca. 60 ppm due to the olefinic carbons is observed, while the <sup>1</sup>H NMR spectra show the corresponding signals for ethylenic protons. For compounds **8a,c**, which possess conformationally flexible phosphite fragments, the four protons appear as a broad signal at 2.8 ppm, while for atropisomeric **8b** the olefinic protons appear as two doublets, with an intensity of two protons for each signal, at 2.3 and 3.0 ppm. These observations account for the fluxional behavior of **8a,c**, which will be discussed below. Moreover, ethylene complexes are capable of exchanging this olefin with propylene, by stirring under an atmosphere of this alkene, to yield complexes **9** (Scheme 5). NMR data for these derivatives show only one group of signals, indicating a fluxional behavior (see below). In addition to the resonances for the PCP fragment, NMR spectra display the expected signals for a propene ligand. For instance, in the <sup>1</sup>H spectrum for **9a** the methyl substituent appears as a doublet at  $\delta$  1.06 ( $J_{\text{HH}} = 5.4$  Hz), while a broad multiplet is observed at  $\delta$  4.39 for the

(18) For comparative purposes, see: Serron, S.; Nolan, S. P.; Moloy, K. G. *Organometallics* **1996**, *15*, 4301.

(19) Salem, H.; Ben-David, Y.; Shimon, L. J. W.; Milstein, D. *Organometallics* **2006**, *25*, 2292.

(20) Weisman, A.; Gozin, M.; Kraatz, H.-B.; Milstein, D. *Inorg. Chem.* **1996**, *35*, 1792.

(21) Conejo, M. M.; Parry, J. S.; Carmona, E.; Schultz, M.; Brennan, J. G.; Beshouri, S. M.; Andersen, R. A.; Rogers, R. D.; Coles, S.; Hurthouse, M. *Chem. Eur. J.* **1999**, *5*, 3000.

(22) Jones, W. D.; Hessel, E. T. *Organometallics* **1990**, *9*, 718.

(23) For other ethylene derivatives with pincer ligands, see: (a) Zhao, J.; Goldman, A. S.; Hartwig, J. F. *Science* **2005**, *307*, 1080. (b) Hahn, C.; Sieler, J.; Taube, R. *Chem. Ber.* **1997**, *130*, 939. (c) Vigalok, A.; Ben-David, Y.; Milstein, D. *Organometallics* **1996**, *15*, 1839. (d) Nemeh, S.; Jensen, C.; Binamira-Soriaga, E.; Kaska, W. C. *Organometallics* **1983**, *2*, 1442. (e) Reference 19.

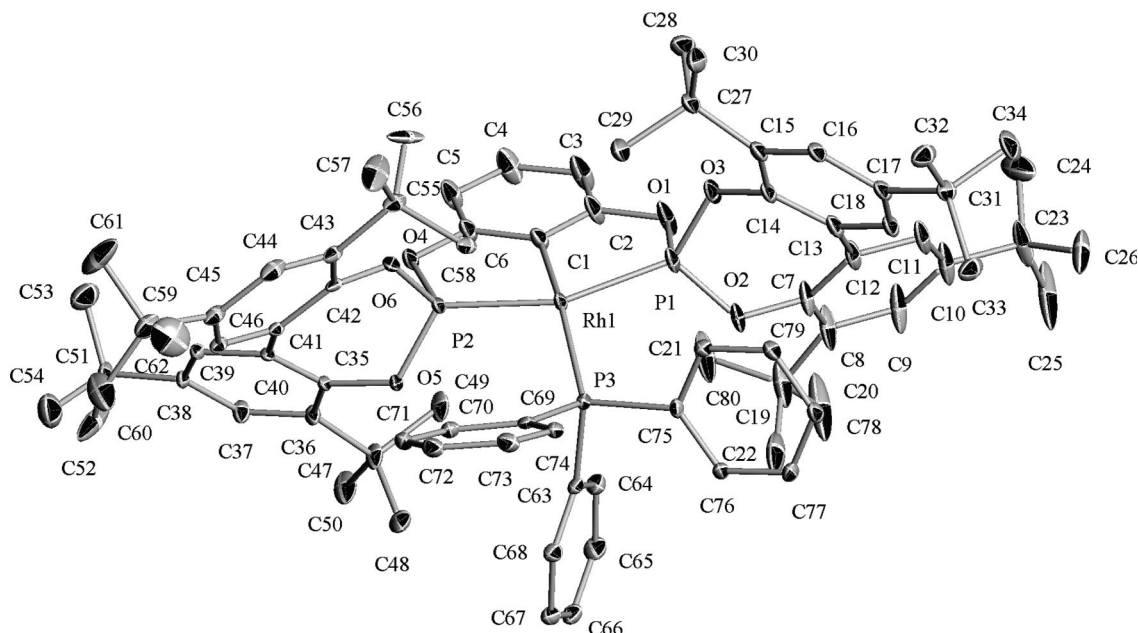


Figure 1. ORTEP perspective of complex **5a**.

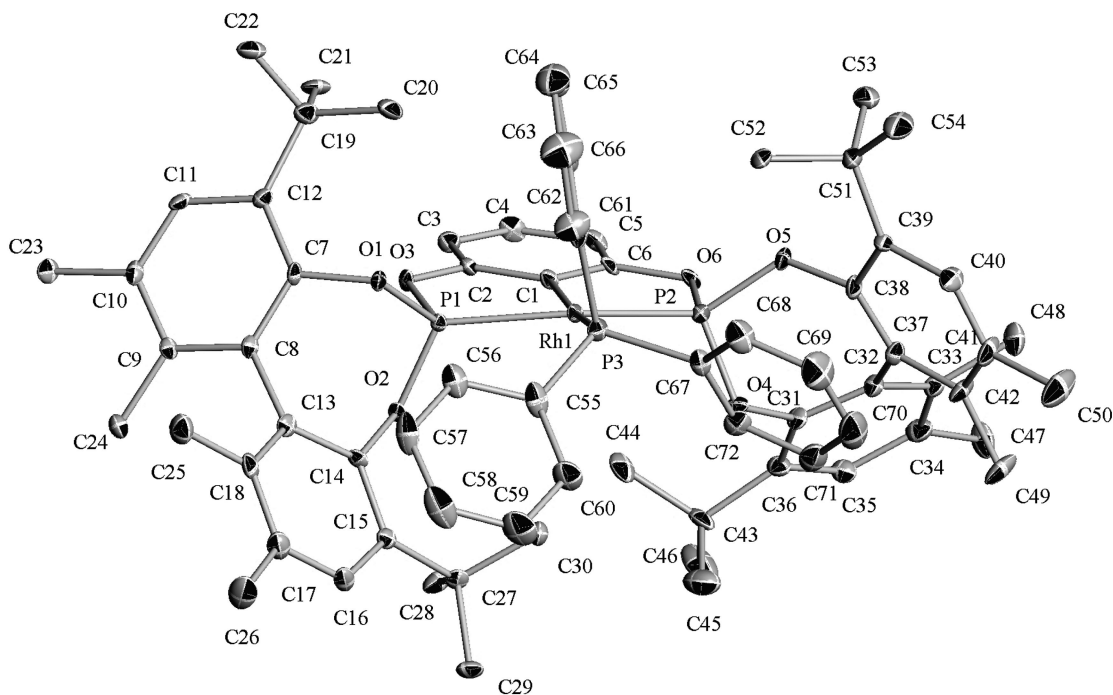


Figure 2. Structure of complex **5b**.

methyne group. Finally, broad doublets at 2.51 ( $J_{\text{HH}} = 8.7$  Hz) and 3.29 ppm ( $J_{\text{HH}} = 12.3$  Hz) are observed for the methylenic protons.

**Structural Characterization of Pincer Complexes.** The observation of an ethylene *ip* coordination in **8a,b** has prompted us to perform a detailed structural study of them, focused at investigating the olefin coordination, using X-ray crystallographic, NMR, and computational techniques.

**(a) Crystallographic Studies.** Complexes **5a–8a**, **5b**, and **8b** have been characterized by single-crystal X-ray crystallography. The corresponding ORTEP diagrams are depicted in Figures 1–6, while in Table 1 are compiled some selected distances and angles for comparative purposes. A comparison of these data indicates that the fragments composed of the metal

and the atoms of the pincer ligand bonded to it are practically superimposable. Moreover, a comparative overview of the structures draws more interesting coincidences among them. First, the magnitude of the angle P–Rh–P lies in the range 153–157°; this angle is substantially smaller than the mean value of ca. 164° found for complexes derived from pincer diphosphines.<sup>24</sup> However, values similar to those found here have also been described in the literature. For instance, a value of 154° has been reported for an *N*-pyrrolyl derivative.<sup>11</sup> Analogously, Ir complexes with diphosphinite pincer ligands

(24) Cambridge Structural Database System, Cambridge Crystallographic Data Centre, 12 Union Road, Cambridge, CB2 1EZ, UK. For QUEST3D search details see the Experimental Section.



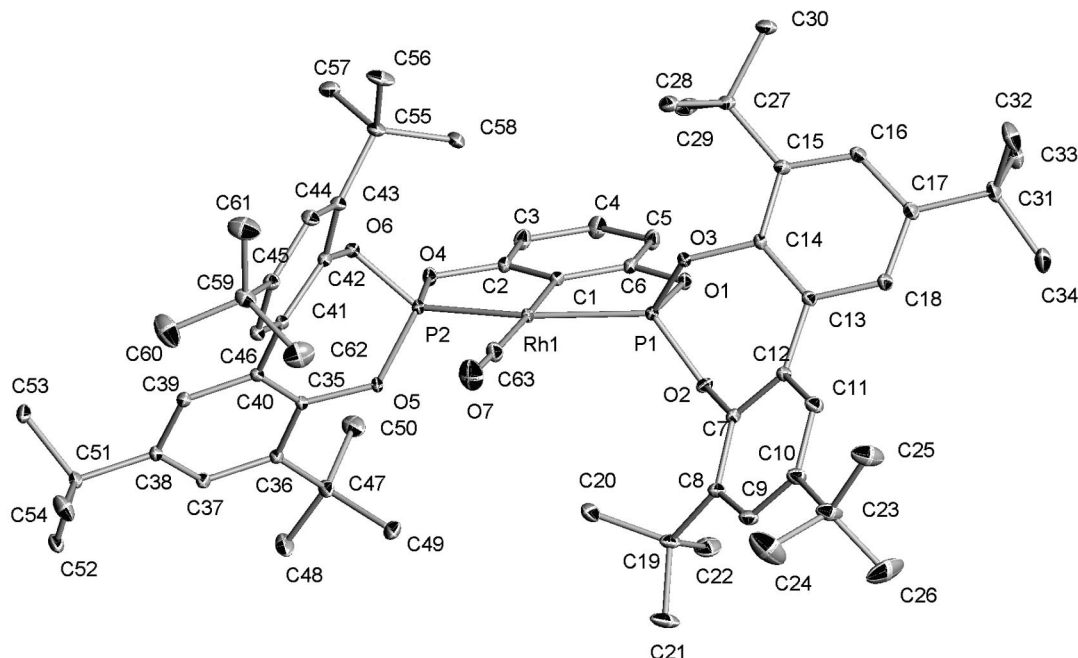


Figure 3. ORTEP view of complex **6a**.

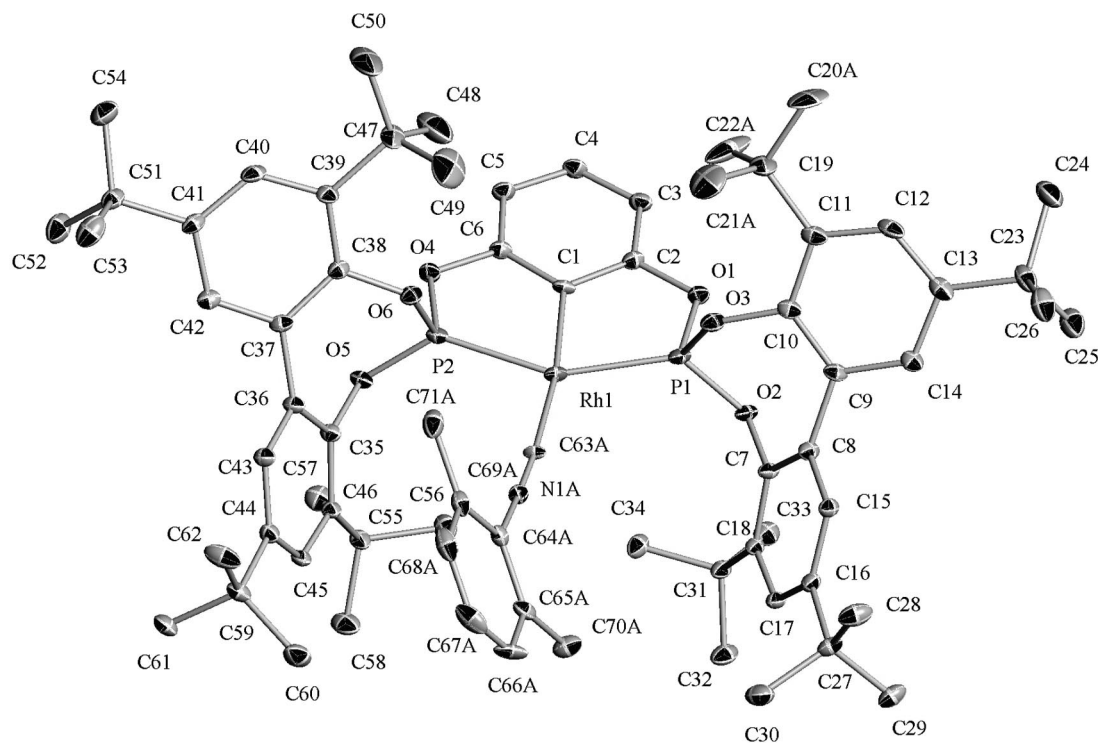


Figure 4. ORTEP perspective of compound **7a**.

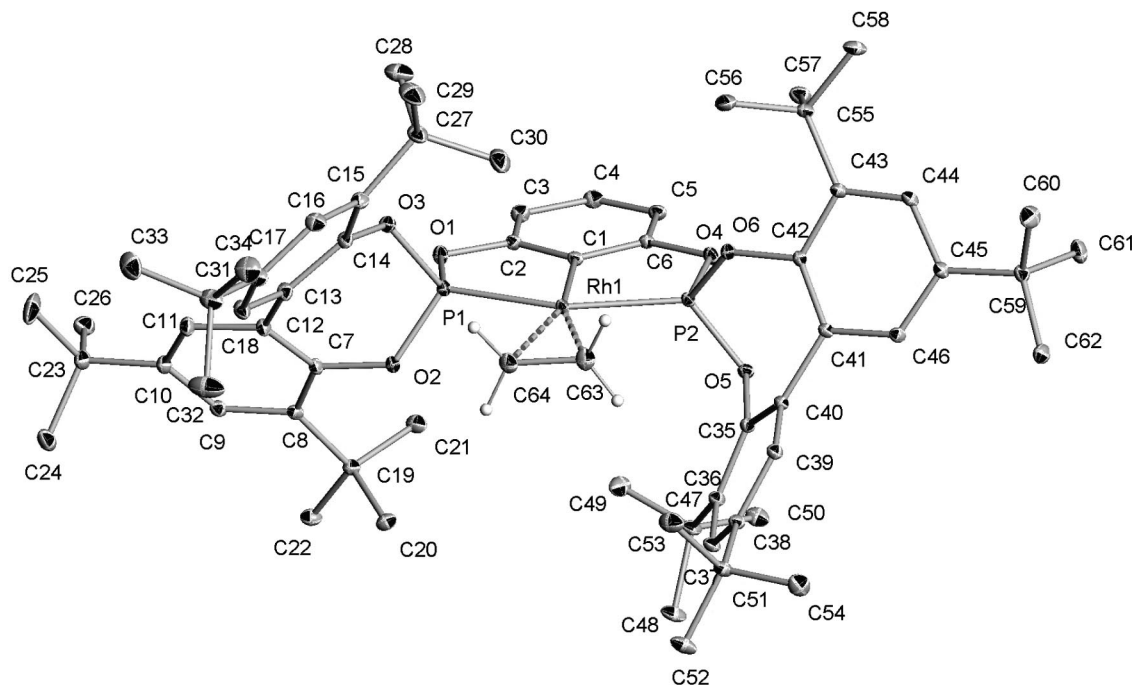
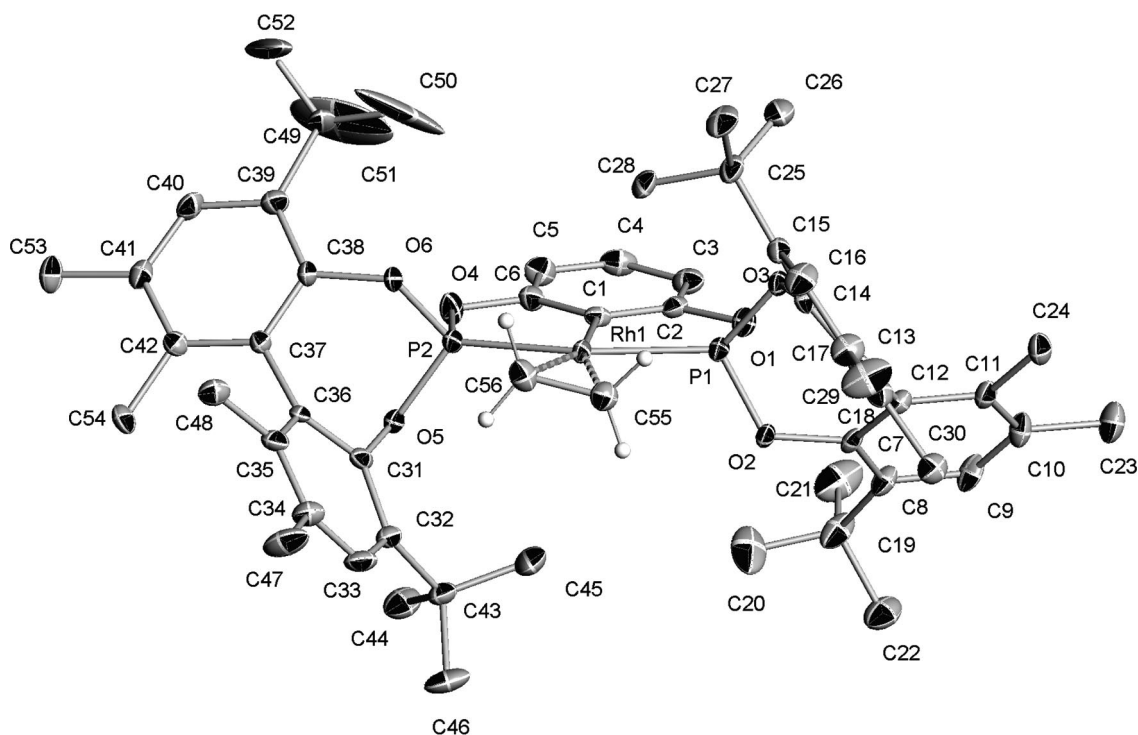
display similar values of this parameter.<sup>19,25</sup> Another remarkable feature of the Rh–PCP fragment along the series is its planarity, which is in contrast with the puckered structures usually

produced by pincer diphosphines.<sup>26</sup> This backbone planarity seems to be caused by the presence of oxygen atoms in the backbone, as other complexes described in the literature derived

(25) (a) Göttker-Schnetmann, I.; White, P.; Brookhart, M. *J. Am. Chem. Soc.* **2004**, *126*, 1804. (b) Göttker-Schnetmann, I.; White, P.; Brookhart, M. *Organometallics* **2004**, *23*, 1766. (c) Sykes, A. C.; White, P.; Brookhart, M. *Organometallics* **2006**, *25*, 1644. (d) Kuklin, S. A.; Sheloumov, A. M.; Dolgushin, F. M.; Ezernitskaya, M. G.; Peregudov, A. S.; Petrovskii, P. V.; Koridze, A. A. *Organometallics* **2006**, *25*, 5466. (e) Denney, M. C.; Pons, V.; Hebden, T. J.; Heinekey, D. M.; Goldberg, K. I. *J. Am. Chem. Soc.* **2006**, *128*, 12048.

(26) For representative examples see: (a) Kraatz, H.-B.; Milstein, D. *J. Organomet. Chem.* **1995**, *488*, 223. (b) Cámpora, J.; Palma, P.; del Río, D.; Alvarez, E. *Organometallics* **2004**, *23*, 1652.

(27) Backbone planarity is not exclusive for oxygen in the backbone, and it also has been observed in pincer bisphosphoramidite complexes. For examples see: (a) Benito-Garagorri, D.; Becker, E.; Wiedermann, J.; Lackner, W.; Pollak, M.; Mereiter, K.; Kisala, J.; Kirchner, K. *Organometallics* **2006**, *25*, 1900. (b) Benito-Garagorri, D.; Bocokic, D.; V.; Mereiter, K.; Kirchner, K. *Organometallics* **2006**, *25*, 3817.

Figure 5. ORTEP view of complex **8a**.Figure 6. ORTEP view of complex **8b**.

from phosphites or phosphinites also show a planar structure of the bridge.<sup>12,25,27</sup>

Another interesting aspect of these structures involves the shape and size of the cavity drawn by the pincer ligand. The first observation is with regard to the conformation of the biphenyls. Complexes derived from the conformationally flexible pincer PCP<sup>a</sup> can adopt a *rac* (corresponding to two enantiomeric C<sub>2</sub>-symmetric Rh–PCP<sup>a</sup> fragments with *S,S* or *R,R* configuration) or a *meso* type conformation, which is characterized by a symmetry plane. Upon these considerations it can be concluded that complexes **6a** and **8a**, which bear the smaller CO and C<sub>2</sub>H<sub>4</sub> ligands, adopt a *rac* conformation. This arrange-

ment is characterized by similar values of  $\alpha$  angles (Figure 7, Table 2) above and below the equatorial plane (i.e.  $\alpha_1$  and  $\alpha_2$  vs  $\alpha_3$  and  $\alpha_4$ , respectively). Otherwise, the magnitude of these parameters is dissimilar in the case of *meso* structures, observed in complexes **5a** and **7a**. Thus,  $\alpha_1$  and  $\alpha_2$  amount for the latter around 31°, while  $\alpha_3$  and  $\alpha_4$  have values around 74°. Moreover, for a *rac* conformation similar values of distances  $d(1-2)$  and  $d(3-4)$  are observed, while these parameters differ in the case of *meso* structures. Therefore, it is apparent that the *meso* conformation is preferred in the case of sterically encumbered compounds. Steric hindrance should be particularly pronounced in complex **5a**, since the ligand PPh<sub>3</sub> is significantly raised over

**Table 1. Selected Structural Parameters of Pincer Complexes<sup>a</sup>**

compd	Rh–P		Rh–C <sub>ipso</sub>	Rh–L	P–Rh–P
<b>4a</b>	2.2705(11)	2.2759(10)	2.033(4)	2.3959(10) <sup>b</sup>	154.55(4)
<b>5a</b>	2.2233(11)	2.2470(11)	2.039(4)	2.3360(11)	155.04(4)
<b>5b</b>	2.2275(12)	2.2629(14)	2.040(5)	2.3572(14)	152.15(5)
<b>6a</b>	2.2245(4)	2.2475(4)	2.0338(16)	1.9069(19)	156.378(16)
<b>7a<sup>c</sup></b>	2.2206(9)	2.2207(10)	2.034(3)	1.991(7)	152.89(3)
				1.949(13)	
<b>8a</b>	2.2076(3)	2.2165(3)	2.0233(12)	2.2184(14)	155.490(13)
				2.2353(14)	
<b>8b</b>	2.2237(7)	2.2096(7)	2.019(3)	2.228(3)	155.37(3)
				2.230(3)	

<sup>a</sup> Angles in deg and distances in Å. <sup>b</sup> L = PPh<sub>3</sub>. <sup>c</sup> Distances for two conformers, modeled due to isonitrile ligand disorder, are given.

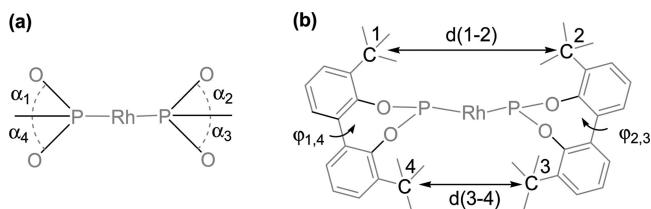


**Figure 7.** Parameters used to compare metal–ligand cavity dimensions: (a)  $\alpha_1$ – $\alpha_4$  angles defined between the P–O bond and the best plane defined by Rh and metal-bonded P and C atoms; (b) torsion angles between biphenyl aryls and distances between quaternary carbons of the *t*-Bu substituents (other aryl substituents have been omitted for clarity).

**Table 2. Cavity Parameters for Rh(PCP)L Complexes<sup>a</sup>**

compd	<i>d</i> (1–2)	<i>d</i> (3–4)	$\alpha_1$	$\alpha_2$	$\alpha_3$	$\alpha_4$	$\varphi_{1,4}$	$\varphi_{2,3}$
<b>4a</b>	7.7	10.0	60.5	55.3	45.6	38.4	48.1	46.9
<b>5a</b>	8.0	9.5	59.6	60.1	41.1	44.5	45.4	47.3
<b>5b</b>	10.2	7.8	32.0	32.6	74.8	76.5	60.4	63.1
<b>6a</b>	8.0	8.8	45.2	49.8	53.4	57.6	45.9	51.6
<b>7a</b>	7.5	8.7	32.5	31.3	75.3	73.1	51.4	50.9
<b>8a</b>	8.0	8.4	48.6	48.8	53.0	52.1	51.6	53.6
<b>8b</b>	8.9	8.2	47.6	48.7	53.8	54.6	62.7	63.5

<sup>a</sup> Angles in deg and distances in Å.

the coordination plane, giving a C(1)–Rh–P(3) angle of 163.2°. It is next interesting to consider complexes **5b** and **8b** derived from enantiopure diphosphite **2b**. Ideally, the corresponding pincer ligand should generate a *C*<sub>2</sub>-symmetric Rh(PCP<sup>b</sup>) fragment. Indeed, this is observed in the case of ethylene derivative **8b** and similar values of *d*(1–2) (8.9 Å) and *d*(3–4) (8.2 Å) are observed. Otherwise, steric hindrance introduced by PPh<sub>3</sub> in **5b** cannot be released by a *meso* structure and a significant distortion from the *C*<sub>2</sub> structure is observed. Thus, the cavity is significantly more opened above the plane (*d*(1–2) = 10.2 Å) than below (*d*(3–4) = 7.8 Å) to accommodate the axial phenyl group. Finally, it is interesting to highlight the differences in torsion angles  $\varphi$  of biphenyls of two types of ligands. Thus, this magnitude amounts to between 40 and 45° for the flexible ligand, while for the chiral ligand, due to the presence of methyl substituents in 6,6'-positions, this angle increases to values of 60 and 63° for **5b** and **8b**, respectively.

Structures of Rh(PCP)L compounds are also of interest due to the magnitude of the Rh–L distance. The distances of the carbonyl and the isonitrile bound to the metal are 1.91 and 1.97 Å, respectively. These distances are longer than those found in related compounds (e.g. 1.86 Å in *trans*-Rh(*p*-tolyl)(CO)-(PPh<sub>3</sub>)<sub>2</sub>,<sup>28a</sup> 1.82 Å in *trans*-RhCl(CO)(PPh<sub>3</sub>)<sub>2</sub>,<sup>28b</sup> or 1.83 Å in *trans*-RhCl(CNXY)(PPri<sub>3</sub>)<sub>2</sub>).<sup>22</sup> Overall, the lengthening of the Rh–L bond can be attributed to the concurrence of two factors, the *trans* influence exerted by the pincer aryl ligand and a

reduced back-bonding ability of the metal center, caused by the  $\pi$ -acidity of the phosphite groups.

Most noteworthy is the fact that coordinated ethylene shows an unexpected in-plane conformation in complexes **8a,b**, with a small angle of 7.4 (**8a**) and 13.0° (**8b**) between planes defined by Rh–PCP and Rh– $\eta^2$ -(C<sub>2</sub>H<sub>4</sub>) fragments. The C=C bond length is similar for **8a** (1.38 Å), while slightly lower for **8b** (1.35 Å), as compared to the mean value observed in other rhodium ethylene derivatives (1.38–1.39 Å).<sup>24</sup> The distance between the ethylene carbons and the Rh atom is 2.23 Å, which is higher than the mean value of 2.13 Å found for rhodium ethylene derivatives and parallels the lengthening of the Rh–L bond observed in complexes **6a** and **7a**.

**(b) NMR Studies of the Olefinic Complexes.** In order to get information about the structural features of the olefinic complexes in solution, we have also studied them by NMR techniques. It has been mentioned above that derivatives of the PCP<sup>a</sup> ligand are fluxional due to an interconversion between *rac* and *meso* conformers; therefore, it is pertinent to consider first the more simple atropisomeric complex **8b**. This compound shows in the <sup>1</sup>H NMR spectrum two filled-in doublets at 2.98 and 2.28 ppm indicative of an AA'XX' spin system for the protons of the ethylene ligand. These signals broaden somewhat on cooling but do not split at the lowest temperature investigated (180 K). Likewise, in the <sup>13</sup>C{<sup>1</sup>H} NMR experiment a slightly broad doublet at 58.6 ppm (*J*<sub>Rh</sub> = 4 Hz) is observed at room temperature for the coordinated olefin. This signal broadens somewhat at lower temperatures. An examination of the 2D NOESY spectrum allows us to differentiate between *t*-Bu groups oriented to the backbone (i.e. those denoted by C(49) and C(19) in Figure 6) and those closer to the olefin. It is worth noting that NOE contacts have been observed between the latter and all ethylene protons.

The *C*<sub>2</sub> symmetry of complex **8b** does not allow us to distinguish between the existence of a single ethylene conformer (*ip* or *u*) or a fast olefin rotation. For that purpose, the less symmetric complex **9b** has also been studied.<sup>29</sup> In this particular case, if the olefin is frozen, the four *tert*-butyl substituents will be nonequivalent, while if there is a fast rotation, according to the NMR time scale, an averaged *C*<sub>2</sub> symmetry is reached and, accordingly, two types of *t*-Bu groups should be observed. Indeed, the latter behavior is observed in both the <sup>1</sup>H and <sup>13</sup>C{<sup>1</sup>H} NMR spectra in the entire temperature range, which is consistent with fast olefin rotation even at 190 K. Therefore, ethylene rotation should also occur in complexes **8**. Upon this assumption, spectra of complexes **8a,c** can be interpreted in terms of an exchange between *rac* and *meso* conformers. Thus, analysis of compound **8a** by <sup>31</sup>P{<sup>1</sup>H} NMR spectroscopy shows at room temperature a doublet at 177.3 ppm (*J*<sub>PRh</sub> = 253 Hz), while cooling of the sample leads to the appearance of a second doublet at 179.2 ppm (<sup>1</sup>*J*<sub>RHP</sub> = 250 Hz) due to a minor species, at a ca. 20:1 rate. On the other hand, in the <sup>1</sup>H NMR region characteristic for a coordinated ethylene, one broad singlet at 2.82 ppm for four protons is observed at room temperature. Upon cooling, this signal splits into two broad signals of equal intensity (e.g. ca. 3.3 and 2.3 ppm at 220 K), while further cooling produces the appearance of an additional broad minor signal at 3.1 ppm. It is interesting to compare these observations with data provided by compound **8c**, which has lower symmetry by virtue of its asymmetric naphthyl backbone. Thus, at room

(28) (a) Krug, C.; Hartwig, J. F. *J. Am. Chem. Soc.* **2002**, *124*, 1674. (b) Rheingold, A. L.; Geib, S. J. *Acta Cryst C* **1987**, *43*, 784.

(29) Cavallo, L.; Cucciolito, M. E.; De Martino, A.; Giordano, F.; Orabona, I.; Vitagliano, A. *Chem. Eur. J.* **2000**, *6*, 1127.



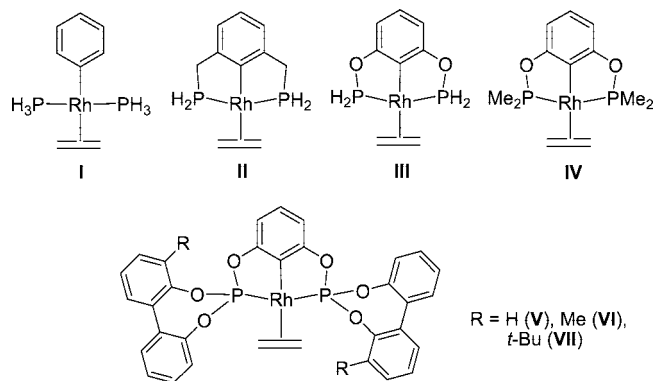


Figure 8. Calculated model complexes.

temperature a broad signal corresponding to all olefinic protons is also observed. However, cooling of the sample produces scission into signals for a major product at 2.2 and 3.2 ppm, while the minor species appears in this case as two broad signals at 2.9 and 3.0 ppm. These observations are in accord with a *rac-meso* exchange in which the *rac* isomer is preferred. The *meso* isomer should give one type of ethylene protons for **8a**, due to the symmetry plane perpendicular to the coordination plane. This plane is absent in **8c**, and accordingly, two types of protons are observed.

These studies demonstrate a facile olefin rotation for complexes **8** in solution. Further support for this phenomenon is provided by theoretical calculations (see below). However, in view of the preferred *ip* conformation detected in the solid state, we have also been interested in providing information about the preferred conformation in solution. For that purpose we have obtained a  $^{13}\text{C}\{^1\text{H}\}$  CP-MAS spectrum of complex **8b**.<sup>30</sup> Interestingly, the spectrum is practically coincident with that obtained in solution (see the Supporting Information). It is worth noting that the olefinic carbons appear in the solid state at 58.6 ppm, while in  $\text{CD}_2\text{Cl}_2$  solution they appear at  $\delta$  58.6 (300 K) or 56.8 (190 K). The similarity is also extended to the phosphorus experiments, as the phosphite groups appear at 175.7 ppm in the  $^{31}\text{P}$  CP-MAS experiment and as a doublet centered at 175.1 ppm ( $J_{\text{RhP}} = 253$  Hz) in the  $^{31}\text{P}\{^1\text{H}\}$  spectrum in solution. These observations indicate an important similarity between the structure of the compound in solution and that in the solid state and suggest that, despite olefin rotation, this ligand is also predominantly located in plane in solution.

**(c) Theoretical Studies.** In order to understand the factors governing olefin conformation in compounds **8**, we have performed DFT calculations (see the Experimental Section for details) on conformers *u* and *ip* of the model complexes **I–VII** (Figure 8). The set of models has been designed with a growing complexity in order to investigate the factors that control the ethylene orientation. Molecules range from the simplest one, **I**, based on monodentate phosphine and phenyl ligands, to the more realistic **VII**, which only differs from complex **8a** in the absence of *t*-Bu groups at the 5- and 5'-positions of the biphenyls, removed for computer limitations. Thus, the significance of the electronic factors has principally been studied by changing the nature of the phosphorus coordinating group in the phosphine (**II**) and phosphinite (**III**, **IV**) models. Alternatively, the influence of steric effects has been scrutinized by modulating the R group at the biphenyl groups (models **V–VII**). Moreover, selected structural parameters for all model complexes have been collected in Tables 3 and 4.

Table 3. Selected Bond Distances and Angles for Compounds **I–IV**<sup>a</sup>

compd	Rh–C <sub>ethylene</sub>	C–C <sub>ethylene</sub>	Rh–P	P–Rh–P	$\alpha(\pi_1/\pi_2)^b$
<i>ip</i> - <b>I</b>	2.335	1.363	2.326	174.6	0
<i>u</i> - <b>I</b>	2.239	1.386	2.308	176.9	90
<i>ip</i> - <b>II</b>	2.260	1.377	2.283	158.5	14.8
<i>u</i> - <b>II</b>	2.249	1.380	2.288	162.6	76.3
<i>ip</i> - <b>III</b>	2.250	1.383	2.260	155.4	0
<i>u</i> - <b>III</b>	2.255	1.379	2.273	157.1	90
<i>ip</i> - <b>IV</b>	2.233	1.387	2.284	156.1	0
<i>u</i> - <b>IV</b>	2.242	1.383	2.291	158.4	90

<sup>a</sup> Angles in deg and distances in Å. <sup>b</sup> Angle between  $\pi_1$  (defined by Rh and pincer ligand atoms bonded to it) and  $\pi_2$  (defined by Rh and ethylene carbons).

Table 4. Selected Bond Distances and Angles for Compounds **V–VII** and **8**<sup>a</sup>

compd	Rh–C <sub>ethylene</sub>	C–C <sub>ethylene</sub>	Rh–P	P–Rh–P	$\alpha(\pi_1/\pi_2)^b$
<i>ip</i> - <b>V</b>	2.286	1.374	2.259	155.1	4.1
<i>u</i> - <b>V</b>	2.282	1.372	2.265	156.9	82.7
<i>ip</i> - <b>VI</b>	2.288	1.374	2.259	155.0	8.8
<i>u</i> - <b>VI</b>	2.284	1.372	2.266	157.9	86.9
<i>ip</i> - <b>VII</b>	2.285	1.373	2.259	155.1	7.9
<b>8a</b>	2.2184(14)	1.377(2)	2.2076(3)	155.490(13)	7.4
	2.2353(14)		2.2165(3)		
<b>8b</b>	2.228(3)	1.353(4)	2.2237(7)	155.37(3)	13.0
	2.230(3)		2.2096(7)		

<sup>a</sup> Angles in deg and distances in Å. <sup>b</sup> Angle between  $\pi_1$  (defined by Rh and pincer ligand atoms bonded to it) and  $\pi_2$  (defined by Rh and ethylene carbons).

Table 5. Relative Energy (kcal mol<sup>−1</sup>) between Isomers of Model Complexes **I–VII**<sup>a</sup>

compd	rel energy <sup>a</sup>
RhPh(PH <sub>3</sub> ) <sub>2</sub> (C <sub>2</sub> H <sub>4</sub> ) ( <b>I</b> )	+10.8
Rh{C <sub>6</sub> H <sub>3</sub> (CH <sub>2</sub> PH <sub>2</sub> ) <sub>2</sub> }(C <sub>2</sub> H <sub>4</sub> ) ( <b>II</b> )	+1.0
Rh{C <sub>6</sub> H <sub>3</sub> (OPH <sub>2</sub> ) <sub>2</sub> }(C <sub>2</sub> H <sub>4</sub> ) ( <b>III</b> )	−0.9
Rh{C <sub>6</sub> H <sub>3</sub> (OPMe <sub>2</sub> ) <sub>2</sub> }(C <sub>2</sub> H <sub>4</sub> ) ( <b>IV</b> )	−0.8
Rh{C <sub>6</sub> H <sub>3</sub> (OP(OC <sub>6</sub> H <sub>4</sub> –OC <sub>6</sub> H <sub>4</sub> ) <sub>2</sub> )(C <sub>2</sub> H <sub>4</sub> ) ( <b>V</b> )	−0.1
Rh{C <sub>6</sub> H <sub>3</sub> (OP(OC <sub>6</sub> H <sub>3</sub> Me–OC <sub>6</sub> H <sub>4</sub> ) <sub>2</sub> )(C <sub>2</sub> H <sub>4</sub> ) ( <b>VI</b> )	−0.6
Rh{C <sub>6</sub> H <sub>3</sub> (OP(OC <sub>6</sub> H <sub>3</sub> – <i>t</i> -Bu–OC <sub>6</sub> H <sub>4</sub> ) <sub>2</sub> )(C <sub>2</sub> H <sub>4</sub> ) ( <b>VII</b> )	<i>b</i>

<sup>a</sup> A negative value for the relative energy indicates that the *ip* conformer is the most stable. <sup>b</sup> *u* conformation cannot be optimized.

As a starting point, the simplest model, RhPh(PH<sub>3</sub>)<sub>2</sub>(C<sub>2</sub>H<sub>4</sub>) (**I**), was computed to confirm in our model system the well-known preference for a *u* orientation of an olefin coordinated to a d<sup>8</sup>-ML<sub>3</sub> fragment and, in addition, to quantify the relative stability between its conformers. As expected, the *u* ethylene conformation is not only preferred but is considerably more stable (10.8 kcal mol<sup>−1</sup>, Table 5) than the *ip* conformation.

We have next analyzed the effect of formally including a bridge between the phenyl and P ligands to compute model complexes **II–IV**. For the phosphine model **II**, the *u* conformation is, as expected, more stable than the *ip* conformation, but only by 1 kcal mol<sup>−1</sup>. Thus, the energy difference has significantly decreased in comparison with model **I**. This effect can be ascribed to the mitigation of the steric pressure produced by a lower P–Rh–P angle in **II** (158.5 and 162.6° for *ip* and *u* conformers, respectively), compared with **I** (174.6 and 176.9° for the *ip* and *u* conformers, respectively). Thus, for the latter, the higher steric pressure exerted by the *cis* coligands in the ethylene *ip* conformer significantly destabilizes it with respect to the *u* conformer.<sup>4</sup> For model complexes **III** and **IV**, in which the P–Rh–P angles are similar to those of **II**, but slightly smaller, the energy difference is also small, although in these cases the *ip* conformation is found to be more stable by about 1 kcal mol<sup>−1</sup>. Interestingly, the presence of O atoms has an important influence on the structure of the metallacycle. As was mentioned, pincer diphosphine ligands are characterized by

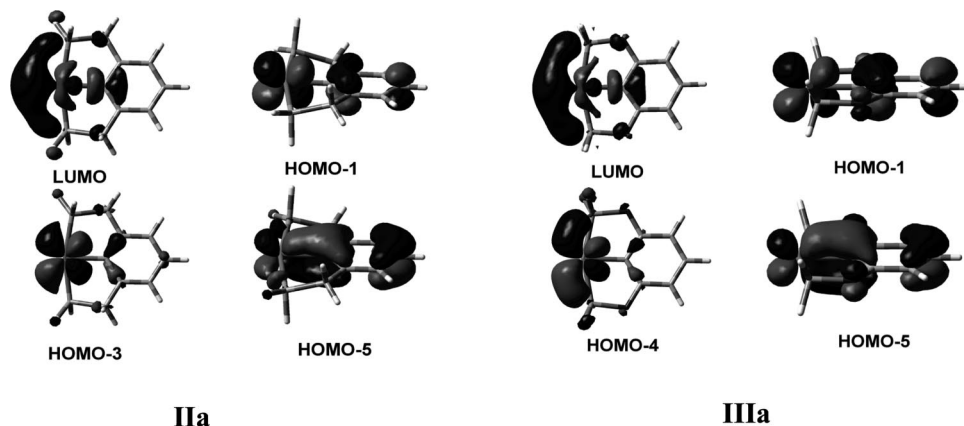
(30) Quan, R. W.; Li, Z.; Jacobsen, E. N. *J. Am. Chem. Soc.* **1996**, *118*, 8156.



Table 6. Summary of Crystallographic Data and Structure Refinement Results from Single-Crystal X-ray Diffraction

	4a	5a	5b	6a	7a	8a	8b
formula	C <sub>80</sub> H <sub>99</sub> O <sub>6</sub> P <sub>3</sub> Rh • C <sub>6</sub> H <sub>14</sub>	C <sub>80</sub> H <sub>98</sub> O <sub>6</sub> P <sub>3</sub> Rh • 0.5C <sub>6</sub> H <sub>14</sub>	2(C <sub>72</sub> H <sub>82</sub> O <sub>6</sub> P <sub>3</sub> Rh) • C <sub>6</sub> H <sub>10</sub> O	2(C <sub>63</sub> H <sub>83</sub> O <sub>7</sub> P <sub>2</sub> Rh) • C <sub>6</sub> H <sub>14</sub> • C <sub>5</sub> H <sub>12</sub>	2(C <sub>71</sub> H <sub>92</sub> NO <sub>6</sub> P <sub>2</sub> Rh) • CHCl <sub>3</sub> • CH <sub>2</sub> Cl <sub>2</sub>	C <sub>64</sub> H <sub>87</sub> O <sub>6</sub> P <sub>2</sub> Rh • C <sub>5</sub> H <sub>12</sub>	C <sub>56</sub> H <sub>71</sub> O <sub>6</sub> P <sub>2</sub> Rh
fw	1474.03	1394.49	2552.51	2392.61	2644.91	1189.33	1004.98
cryst syst	triclinic	triclinic	monoclinic	monoclinic	triclinic	monoclinic	orthorhombic
space group	<i>P</i> $\bar{1}$	<i>P</i> $\bar{1}$	<i>C</i> 2	<i>P</i> 2 <sub>1</sub> / <i>c</i>	<i>P</i> $\bar{1}$	<i>P</i> 2 <sub>1</sub> / <i>c</i>	<i>P</i> 2 <sub>1</sub> 2 <sub>1</sub>
<i>a</i> , Å	13.4989(8)	14.4920(18)	24.7253(9)	12.3963(2)	12.6244(9)	17.2239(5)	10.4092(11)
<i>b</i> , Å	16.7201(9)	17.417(2)	12.9836(4)	19.8113(4)	18.5218(15)	19.2234(6)	18.8544(18)
<i>c</i> , Å	19.3595(11)	19.351(2)	21.7178(6)	27.2608(6)	18.850(2)	20.3456(6)	26.636(3)
$\alpha$ , deg	110.784(3)	65.484(5)	90	90	106.614(3)	90	90
$\beta$ , deg	96.741(3)	69.097(5)	99.008(2)	95.0850(10)	108.221(3)	97.7050(10)	90
$\gamma$ , deg	97.170(3)	70.040(5)	90	90	107.806(2)	90	90
cell vol, Å <sup>3</sup>	3991.2(4)	4042.7(8)	6885.9(4)	6668.5(2)	3614.0(6)	6675.6(3)	5227.6(9)
<i>Z</i>	2	2	2	2	1	4	4
$\rho_{\text{calcd}}$ , Mg/m <sup>3</sup>	1.227	1.146	1.231	1.192	1.215	1.183	1.277
cryst color	yellow	orange	yellow	yellow	yellow	orange	orange
$\mu$ , mm <sup>-1</sup>	0.358	0.318	0.368	0.353	0.421	0.351	0.436
<i>F</i> (000)	1568	1482	2692	2552	1396	2544	2120
no. of measd rflns	49 365	117 604	49 957	110 399	56 585	153 626	45 841
no. of indep rflns	24 502	18 888	16 411	20 357	21 952	20 381	11 402
no. of params	874	865	783	732	917	719	602
R1( <i>F</i> ) ( <i>F</i> <sup>2</sup> > 2 $\sigma$ ( <i>F</i> <sup>2</sup> )) <sup>a</sup>	0.0589	0.0613	0.0711	0.0373	0.0680	0.0311	0.0352
wR2( <i>F</i> <sup>2</sup> ) <sup>b</sup> (all data)	0.1651	0.1788	0.1561	0.0934	0.2169	0.0797	0.0717
<i>S</i> <sup>c</sup> (all data)	1.016	1.020	1.047	1.056	1.043	1.052	1.019
Flack param			0.03(3)				-0.018(17)

<sup>a</sup>  $R1(F) = \sum(F_o - F_c)/\sum F_o$  for the observed reflections ( $F^2 > 2\sigma(F^2)$ ). <sup>b</sup>  $wR2(F^2) = \{\sum[w(F_o^2 - F_c^2)^2]/\sum w(F_o^2)^2\}^{1/2}$ . <sup>c</sup>  $S = \{\sum[w(F_o^2 - F_c^2)^2]/(n - p)\}^{1/2}$  ( $n$  = number of reflections,  $p$  = number of parameters).

Figure 9. Selected 3D isosurfaces corresponding to the MOs of fragments **IIa** and **IIIa**.

puckered structures, while pincer diphosphite complexes described here possess a planar structure. This difference is well reproduced in the series of models **II**–**IV**. Thus, phosphinito models **III** and **IV** (as well as **V**–**VII**, see below) describe planar structures, while a puckered arrangement is evident in the structures of isomers of model **II**.

With the aim of rationalizing the effect caused by the formal substitution of a CH<sub>2</sub> group by an O atom, we have analyzed the MOs of the rhodium–pincer ligand fragments of **II** and **III**, namely **IIa** and **IIIa**, respectively. The two interactions between the ethylene ligand and the metallic fragment are well-known: (i) donation from ethylene to the LUMO of the fragment (the typical empty hybrid of a d<sup>8</sup>-ML<sub>3</sub> FMO, Figure 9) and (ii) back-donation from d<sub>xy</sub> or from d<sub>xz</sub> orbitals for the *ip* and *u* isomers (the coordination plane is *xy*), respectively. Concerning the donation, the involvement of Rh in the LUMO in the fragments **IIa** and **IIIa** is the same (47%), but the contribution from the P atoms to the LUMO is higher in **IIIa** (39%) than in **IIa** (31%). Thus, the resulting lobes of the LUMO in **IIIa** are to some extent better adapted, in terms of overlap, for receiving the donation of the occupied ethylene orbital if the in-plane conformation is attained than those of **IIa**. Concerning the back-donation, there are two orbitals that are appropriate for such an interaction, one

for the in-plane conformer (HOMO-3 in **IIa** and HOMO-4 in **IIIa**) and the other for the *u* species (HOMO-1 for both **IIa** and **IIIa**). HOMO-5 corresponds to the bonding combination of the d<sub>xz</sub> orbital with the p orbitals of the aromatic ring. The back-donation in fragment **IIa** is favored for the *u* isomer, with respect to **IIIa**, because the participation of the Rh d<sub>xz</sub> orbital in HOMO-1 is 78%, higher than the Rh character of 58% found in the HOMO-1 of **IIIa**. In contrast, in fragment **IIIa** HOMO-4 is formed mainly by the Rh d<sub>xy</sub> orbital (75% Rh character) with an important participation from the P atoms (21%). This contribution expands the lobes of the orbital on the appropriate way to favor the back-donation in the in-plane isomer. This situation is somewhat disfavored for **IIa**, where the analogous orbital, HOMO-3, presents an 83% Rh character, with a small contribution (6%) from the P atoms. Summarizing, there is a subtle electronic effect associated with the formal substitution of a CH<sub>2</sub> group by an O atom. On the basis of the Rh contributions to the frontier FMOs and their corresponding topologies, we can expect a better preference for the *ip* conformer in **IIIa** than in **IIa**.

Interestingly, the analysis of the rotational barrier of the ethylene ligand in compounds **II** and **III** (see the Supporting Information) corroborates the above discussion. The barrier is

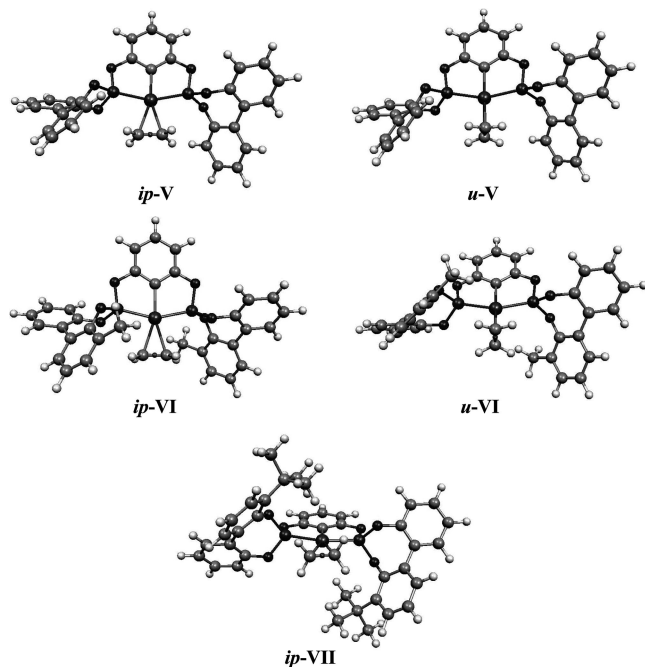


**Figure 10.** Optimized structures of conformers of the model complexes **V–VII**.

small in both cases (ca. 1 kcal mol<sup>−1</sup>), in good agreement with a relatively minor  $\pi$  contribution to the Rh–ethylene bond, which would facilitate the rotation of the olefin.

The importance of steric factors produced by the substituents of the biphenyl ring has been studied by calculating the model complexes Rh{C<sub>6</sub>H<sub>3</sub>(OP(OC<sub>6</sub>H<sub>3</sub>R-OC<sub>6</sub>H<sub>4</sub>)<sub>2</sub>)(C<sub>2</sub>H<sub>4</sub>) (R = H (**V**), Me (**VI**), *t*-Bu (**VII**)). For models **V** and **VI**, both *u* and *ip* conformations have been located as stationary points (Figure 10). The computed energies for isomers of **V** and **VI** are quite similar (Table 5). For model **VI** the *ip* conformation is more stable with respect to the *u* isomer by only 0.6 kcal mol<sup>−1</sup>, while for **V** the *ip* conformation is more stable by no more than 0.1 kcal mol<sup>−1</sup>. For complex **VII**, although different conformations for the ethylene ligand were explored as starting geometries, the only conformation that appears to be a stationary point corresponds to the *ip* isomer. All our attempts of optimization of the *u* conformer converged into the *ip* conformer. Interestingly, the structural parameters of the computed model **VII** are in good agreement with the experimental data of compound **8a**. For instance, the calculated parameters around the Rh–C<sub>2</sub>H<sub>4</sub> moiety (Rh–C = 2.285 Å and C–C = 1.373 Å) agree well with the experimental values (Rh–C = 2.235(2) and 2.218(2) Å and C–C = 1.377(2) Å). Likewise, there is a good accord in the values of the P–Rh–P angle (experimental, 155.5°; computed, 155.1°). The calculations are also capable of describing the small deviation of the Rh–C<sub>2</sub>H<sub>4</sub> plane with respect to the Rh–PCP plane (experimental, 7.4°; computed, 7.9°). Finally, the calculation reproduces well the planarity of the Rh–PCP fragment of **8a**.

From comparison of models **V–VII** it appears that the bulky *t*-Bu groups have a decisive role in destabilizing the *u* conformer. This effect can be readily seen using space-filling models of *u*-**VI**, *ip*-**VI**, and *ip*-**VII** complexes (see the Supporting Information). A comparison of conformers of **VI** show that the cavity generated by the metal and the pincer ligand is practically superimposable and can allocate the ethylene in either conformation without distortion. Otherwise, the presence of *t*-Bu groups in **VII** does not increase encumbrance in the coordination

plane but offers an important steric hindrance in a perpendicular direction to this plane. Thus, an ethylene ligand can be easily coordinated in a *ip* fashion, but a *u* orientation would require a distortion of the cavity. This fact is apparently in contradiction with the observed olefin rotation process. However, comparison of structures of complexes **5b** and **8b** reveal the ability of the pincer ligand to distort and generate a more opened cavity which will be able to accommodate transiently the ethylene in a *u* conformation.

## Conclusions

A series of rhodium complexes derived from pincer diphosphite and neutral L ligands has been prepared and characterized. IR studies of the carbonyl (**6a**) and isonitrile (**7a**) complexes show the  $\pi$ -acceptor ability of the pincer diphosphite ligand. Comparison of structures of complexes **5a–8a**, **5b**, and **8b** indicate very similar parameters for the Rh–PCP fragment in the coordination plane. In addition, in the series of derivatives of the conformationally flexible ligand PCP<sup>a</sup>, it has been observed that the conformation of the biphenyl groups is determined by the size of the L ligand. Thus, a *rac* conformation has been observed for less demanding groups, while the *meso* structure is preferred for larger L ligands. Moreover, *rac–meso* isomerization has been observed for these complexes in solution. Most noteworthy, X-ray structural determination of complexes **8** indicate a rare in-plane conformation of the ethylene ligand. NMR studies indicate that olefin complexes (**8** and **9**) have a fluxional behavior caused by a olefin rotation process, which could not be frozen at the lower temperature investigated. Moreover, <sup>13</sup>C{<sup>1</sup>H} NMR spectra of **8b** in solution and in the solid state practically match, thus indicating an important coincidence between solid-state and solution structures for this complex.

To complete the experimental studies, detailed computational investigations of *u* and *ip* conformers of a set of model complexes **I–VII** have been performed. An investigation of electronic effects indicates that the nature of the P-fragments (phosphine vs phosphinite) do not play an important role in altering the relative stabilities of both types of conformers. Otherwise, steric effects play a decisive influence on olefin conformation. Two different effects have been identified. First, the reduction of the P–Rh–P angle, as compared with the ideal for two trans-coordinated ligands, causes the reduction of hindrance toward the remaining coordination position. The second is with regard to the size of the R substituents at the 3- and 3'-positions of the biphenyl fragments. Thus, while for H and Me derivatives both conformers are of similar energy, the cavity outlined by the *t*-Bu-substituted pincer ligand in model **VII** significantly reduces the available space above and below the coordination plane, favoring the *ip* conformation.

## Experimental Section

**General Comments.** All reactions and manipulations were performed under nitrogen or argon, either in a Braun Labmaster 100 glovebox or using standard Schlenk-type techniques. All solvents were distilled under nitrogen using the following dessicants: sodium benzophenone ketyl for benzene, diethyl ether (Et<sub>2</sub>O), and tetrahydrofuran (THF), sodium for petroleum ether and toluene, CaH<sub>2</sub> for dichloromethane (CH<sub>2</sub>Cl<sub>2</sub>), and NaOMe for methanol (MeOH). Chlorophosphites **1**<sup>31</sup> and the complex Rh(Cl)(PPh<sub>3</sub>)<sub>3</sub><sup>32</sup>

(31) (a) Buisman, G. J. H.; Kamer, P. C. J.; van Leeuwen, P. W. N. M. *Tetrahedron: Asymmetry* **1993**, *4*, 1625. (b) Suárez, A.; Méndez-Rojas, M. A.; Pizzano, A. *Organometallics* **2002**, *21*, 4611.

were prepared according to literature procedures. NMR spectra were obtained on Bruker DPX-300, DRX-400, and DRX-500 spectrometers.  $^{31}\text{P}\{^1\text{H}\}$  NMR shifts were referenced to external 85%  $\text{H}_3\text{PO}_4$ , while  $^{13}\text{C}\{^1\text{H}\}$  and  $^1\text{H}$  shifts were referenced to the residual signals of deuterated solvents. All data are reported in ppm downfield from  $\text{Me}_4\text{Si}$ . HRMS data were obtained using a Jeol JMS-SX 102A mass spectrometer at the Analytical Services of the Universidad de Sevilla (CITIUS). Elemental analyses were run by the Analytical Service of the Instituto de Investigaciones Químicas.

**$\mu$ -1,3-Phenylenebis[1,1'-(3,3',5,5'-tetra-*tert*-butyl)biphen-2,2'-diyl]diphosphite (2a).** Over a solution of phosphorochloridite **1a** (4.74 g, 10 mmol) and  $\text{NEt}_3$  (1.5 mL, 11 mmol) in THF (40 mL) was slowly added a resorcinol (0.55 g, 5 mmol) solution in the same solvent (40 mL). After the mixture was stirred for 16 h, the solvent was evaporated, the residue treated with  $\text{Et}_2\text{O}$  (3 50 mL), and this mixture filtered through a pad of neutral alumina. Removal of the solvent yielded compound **2a** as a white foamy solid (4.29 g, 87%).  $^1\text{H}$  NMR ( $\text{CDCl}_3$ , 400 MHz):  $\delta$  1.36 (s, 36H, 4  $\text{CMe}_3$ ), 1.48 (s, 36H, 4  $\text{CMe}_3$ ), 6.80 (dd,  $^3J_{\text{HH}} = 8.4$  Hz,  $^4J_{\text{HH}} = 2.5$  Hz, 2H, 2 H arom), 6.92 (m, 1H, H arom), 7.16 (t,  $^3J_{\text{HH}} = 8.4$  Hz, 1H, H arom), 7.20 (d,  $^4J_{\text{HH}} = 2.4$  Hz, 4H, 4 H arom), 7.45 (d,  $^4J_{\text{HH}} = 2.4$  Hz, 4H, 4 H arom).  $^{31}\text{P}\{^1\text{H}\}$  NMR ( $\text{CDCl}_3$ , 202.4 MHz):  $\delta$  137.9 (s).  $^{13}\text{C}\{^1\text{H}\}$  NMR ( $\text{CDCl}_3$ , 100.6 MHz):  $\delta$  31.3 (br s, 4  $\text{CMe}_3$ ), 31.5 (s, 4  $\text{CMe}_3$ ), 34.7 (4  $\text{CMe}_3$ ), 35.5 (4  $\text{CMe}_3$ ), 112.8 (t,  $J_{\text{PC}} = 8$  Hz, CH arom), 115.8 (d,  $J_{\text{PC}} = 9$  Hz, 2 CH arom), 124.4 (s, 4 CH arom), 126.6 (s, 4 CH arom), 130.0 (s, CH arom), 132.8 (d,  $J_{\text{PC}} = 2$  Hz, 4  $\text{C}_q$  arom), 140.3 (s, 4  $\text{C}_q$  arom), 145.3 (d,  $J_{\text{PC}} = 6$  Hz, 4  $\text{C}_q$  arom), 146.8 (s, 4  $\text{C}_q$  arom), 153.2 (d,  $J_{\text{PC}} = 7$  Hz, 2  $\text{C}_q$  arom). HRMS (FAB):  $m/z$  986.5755,  $[\text{M}]^+$  (exact mass calcd for  $\text{C}_{62}\text{H}_{84}\text{O}_6\text{P}_2$  986.5743).

**(*R,R*)- $\mu$ -1,3-phenylenebis[1,1'-(3,3'-di-*tert*-butyl-5,5',6,6'-tetramethyl)biphen-2,2'-diyl]diphosphite (2b).** Compound **2b** has been obtained as a white solid as described for **2a** but starting from chlorophosphite **1b** (1.70 g, 78%).  $[\alpha]_{\text{D}}^{20} = -347$  (c 1.0, THF).  $^1\text{H}$  NMR ( $\text{CDCl}_3$ , 500 MHz):  $\delta$  1.41 (s, 18H, 2  $\text{CMe}_3$ ), 1.42 (s, 18H, 2  $\text{CMe}_3$ ), 1.82 (s, 6H, 2 Me), 1.83 (s, 6H, 2 Me), 2.23 (s, 6H, 2 Me), 2.26 (s, 6H, 2 Me), 6.80 (m, 3H, 3 H arom), 7.14 (t,  $J_{\text{HH}} = 7.5$  Hz, 1H, H arom), 7.16 (s, 4H, 4 H arom).  $^{31}\text{P}\{^1\text{H}\}$  NMR ( $\text{CDCl}_3$ , 121.5 MHz):  $\delta$  132.6 (s).  $^{13}\text{C}\{^1\text{H}\}$  NMR ( $\text{CDCl}_3$ , 75.5 MHz):  $\delta$  16.9 (s, 2 Ar-Me), 17.1 (s, 2 Ar-Me), 20.7 (s, 4 Ar-Me), 31.5 (s,  $\text{CMe}_3$ ), 31.5 (s,  $\text{CMe}_3$ ), 32.0 (s, 2  $\text{CMe}_3$ ), 34.9 (s, 2  $\text{CMe}_3$ ), 35.1 (s, 2  $\text{CMe}_3$ ), 112.6 (t,  $J_{\text{PC}} = 9$  Hz, CH arom,  $\text{C}^\circ$ ), 115.6 (d,  $J_{\text{PC}} = 10$  Hz, 2 CH arom), 128.1 (s, 2 CH arom), 128.5 (s, 2 CH arom), 130.2 (s, CH arom), 130.7 (br s, 2  $\text{C}_q$  arom), 132.3 (m, 2  $\text{C}_q$  arom), 132.4 (s, 2  $\text{C}_q$  arom), 133.2 (s, 2  $\text{C}_q$  arom), 134.7 (s, 2  $\text{C}_q$  arom), 135.5 (s, 2  $\text{C}_q$  arom), 137.7 (s, 2  $\text{C}_q$  arom), 138.5 (br s, 2  $\text{C}_q$  arom), 144.7 (d,  $J_{\text{PC}} = 6$  Hz, 2  $\text{C}_q$  arom), 144.8 (s, 2  $\text{C}_q$  arom), 153.6 (d,  $J_{\text{PC}} = 9$  Hz, 2  $\text{C}_q$  arom). HRMS (FAB):  $m/z$  875.4586,  $[\text{M} + \text{H}]^+$  (exact mass calcd for  $\text{C}_{54}\text{H}_{69}\text{O}_6\text{P}_2$  875.4569).

**$\mu$ -1,3-Naphthalenediylbis[1,1'-(3,3',5,5'-tetra-*tert*-butyl)biphen-2,2'-diyl]diphosphite (2c).** Over a solution of phosphorochloridite **1a** (1.48 g, 3.1 mmol) and  $\text{NEt}_3$  (0.5 mL, 3.1 mmol) in THF (25 mL) was slowly added a 1,3-dihydroxynaphthalene (0.250 g, 1.6 mmol) solution in the same solvent (15 mL). After the mixture was stirred for 16 h, the solvent was evaporated and the residue was extracted with  $\text{Et}_2\text{O}$  (3  $\times$  20 mL) and filtered through a pad of neutral alumina. Removal of the solvent yielded compound **2c** as a white foamy solid (1.46 g, 90%).  $^1\text{H}$  NMR ( $\text{CDCl}_3$ , 400 MHz):  $\delta$  1.35 (s, 18H, 2  $\text{CMe}_3$ ), 1.36 (s, 18H, 2  $\text{CMe}_3$ ), 1.39 (s, 18H, 2  $\text{CMe}_3$ ), 1.50 (s, 18H, 2  $\text{CMe}_3$ ), 7.09 (s, 1H, H arom), 7.21 (d,  $^4J_{\text{HH}} = 2.4$  Hz, 2H, 2 H arom), 7.22 (d,  $^4J_{\text{HH}} = 2.4$  Hz, 2H, 2 H arom), 7.24 (s, 1H, H arom), 7.28 (m, 1H, H arom), 7.41 (m, 1H, H arom), 7.44 (d,  $^4J_{\text{HH}} = 2.4$  Hz, 2H, 2 H arom), 7.46 (d,  $^4J_{\text{HH}} = 2.4$  Hz, 2H, 2 H arom), 7.61 (d,  $^3J_{\text{HH}} = 8.0$  Hz, 1H, H arom), 7.97 (d,  $^3J_{\text{HH}}$

$= 9.3$  Hz, 1H, H arom).  $^{31}\text{P}\{^1\text{H}\}$  NMR ( $\text{CDCl}_3$ , 162.1 MHz):  $\delta$  136.9 (s), 138.9 (s).  $^{13}\text{C}\{^1\text{H}\}$  NMR ( $\text{CDCl}_3$ , 125.8 MHz):  $\delta$  31.2 (s, 2  $\text{CMe}_3$ ), 31.3 (s, 2  $\text{CMe}_3$ ), 31.6 (s, 4  $\text{CMe}_3$ ), 34.7 (s, 4  $\text{CMe}_3$ ), 35.4 (s, 2  $\text{CMe}_3$ ), 35.5 (s, 2  $\text{CMe}_3$ ), 110.7 (dd,  $J_{\text{CP}} = 13$  Hz,  $J_{\text{CP}} = 5$  Hz, CH arom), 112.3 (d,  $J_{\text{CP}} = 12$  Hz, CH arom), 122.9 (s, CH arom), 124.4 (s, 2 CH arom), 124.5 (s, 2 CH arom), 124.8 (s, CH arom), 126.7 (s, 4 CH arom), 127.0 (s, CH arom), 127.3 (s, CH arom), 132.8 (s, 5  $\text{C}_q$ ), 134.7 (s,  $\text{C}_q$ ), 140.3 (s, 2  $\text{C}_q$ ), 140.4 (s, 2  $\text{C}_q$ ), 145.5 (s, 4  $\text{C}_q$ ), 146.8 (s, 2  $\text{C}_q$ ), 146.9 (s, 2  $\text{C}_q$ ), 149.3 (d,  $J_{\text{CP}} = 12$  Hz,  $\text{C}_q$ ), 149.5 (d,  $J_{\text{PC}} = 12$  Hz,  $\text{C}_q$ ). HRMS (FAB):  $m/z$  1059.5857,  $[\text{M} + \text{Na}]^+$  (exact mass calcd for  $\text{C}_{66}\text{H}_{86}\text{O}_6\text{P}_2\text{Na}$ : 1059.5797).

**$\text{Rh}(\text{H})(\text{Cl})(\text{PCP}^a)(\text{PPh}_3)$  (4a).** Although this compound was first observed in the reaction between  $\text{Rh}(\text{Cl})(\text{PPh}_3)_3$  and **2a**, it is more conveniently obtained by protonation of **5a**. Over a solution of **5a** (0.11 g, 0.081 mmol) in THF (10 mL) was added HCl (0.2 mL, 1.0 M in  $\text{Et}_2\text{O}$ ). The mixture was stirred vigorously for 24 h, the solvent evaporated, and the remaining residue extracted with *n*-hexane (3  $\times$  10 mL). Solvent evaporation yields **4a** as a yellow solid (0.09 g, 80%). IR (Nujol mull,  $\text{cm}^{-1}$ ): 2112 (m,  $\nu_{\text{RhH}}$ ).  $^1\text{H}$  NMR ( $\text{CDCl}_3$ , 500 MHz):  $\delta$  -15.63 (dq,  $J_{\text{HRh}} = J_{\text{HPo}} = J_{\text{HP}} = 12$  Hz, 1H, Rh-H), 1.22 (s, 18H, 2  $\text{CMe}_3$ ), 1.27 (s, 18H, 2  $\text{CMe}_3$ ), 1.32 (s, 18H, 2  $\text{CMe}_3$ ), 1.42 (s, 18H, 2  $\text{CMe}_3$ ), 6.63 (dd,  $J_{\text{HH}} = 8$  Hz,  $J_{\text{RhH}} = 2$  Hz, 2H, 2 H arom), 6.84 (m, 6H, 6 H arom,  $\text{PPh}_3$ ), 6.85 (m, 2H, 2 H arom), 6.91 (d,  $J_{\text{HH}} = 2$  Hz, 2H, 2 H arom), 6.95 (t,  $J_{\text{HH}} = 8$  Hz, 1H, H arom), 6.98 (t,  $J_{\text{HH}} = 7.5$  Hz, 3H, 3 H arom,  $\text{PPh}_3$ ), 7.17 (dd,  $J_{\text{HH}} = 7.5$  Hz,  $J_{\text{HP}} = 10$  Hz, 6H, 6 H arom,  $\text{PPh}_3$ ), 7.33 (m, 2H, 2 H arom), 7.37 (d,  $J_{\text{HH}} = 2$  Hz, 2H, 2 H arom).  $^{31}\text{P}\{^1\text{H}\}$  NMR ( $\text{C}_6\text{D}_6$ , 162.1 MHz):  $\delta$  14.7 (dt,  $J_{\text{PRh}} = 87$  Hz,  $J_{\text{PP}} = 35$  Hz, P-C), 148.9 (dd,  $J_{\text{PRh}} = 178$  Hz, P-O).  $^{13}\text{C}\{^1\text{H}\}$  NMR ( $\text{CDCl}_3$ , 75.5 MHz):  $\delta$  31.6 (s, 2  $\text{CMe}_3$ ), 31.6 (s, 2  $\text{CMe}_3$ ), 31.7 (s, 2  $\text{CMe}_3$ ), 32.0 (s, 2  $\text{CMe}_3$ ), 34.8 (s, 4  $\text{CMe}_3$ ), 35.7 (s, 2  $\text{CMe}_3$ ), 36.1 (s, 2  $\text{CMe}_3$ ), 106.8 (t,  $J_{\text{PC}} = 7$  Hz, 2 CH arom), 124.6 (s, 2 CH arom), 125.0 (s, 2 CH arom), 126.8 (s, CH arom), 127.3 (s, 2 CH arom), 127.8 (d,  $J_{\text{PC}} = 9$  Hz, 6 CH arom,  $\text{PPh}_3$ ), 128.3 (s, 2 CH arom), 129.1 (s, 3 CH arom), 129.9 (s, 2  $\text{C}_q$  arom), 131.6 (s, 2  $\text{C}_q$  arom), 133.4 (d,  $J_{\text{PC}} = 12$  Hz, 6 CH arom), 134.6 (d,  $J_{\text{PC}} = 35$  Hz, 3  $\text{C}_q$  arom), 136.5 (m,  $\text{C}_q$  arom), 139.7 (s, 2  $\text{C}_q$  arom), 141.2 (s, 2  $\text{C}_q$  arom), 145.6 (br s, 2  $\text{C}_q$  arom), 146.4 (s, 2  $\text{C}_q$  arom), 146.8 (s, 2  $\text{C}_q$  arom), 147.4 (t,  $J_{\text{PC}} = 7$  Hz, 2  $\text{C}_q$  arom), 156.0 (t,  $J_{\text{PC}} = 11$  Hz, 2  $\text{OC}_q$  arom). Anal. Calcd for  $\text{C}_{80}\text{H}_{99}\text{ClO}_6\text{P}_3\text{Rh}$ : C, 69.2; H, 7.2. Found: C, 69.3; H, 7.6.

**$\text{Rh}(\text{PCP}^a)(\text{PPh}_3)$  (5a).** Over a suspension of  $\text{RhCl}(\text{PPh}_3)_3$  (0.46 g, 0.5 mmol) in THF (5 mL) was added diphosphite **2a** (0.49 g, 0.5 mmol) dissolved in THF (10 mL). The mixture was heated over 24 h at 70  $^\circ\text{C}$ . An excess of  $\text{NEt}_3$  (0.1 mL) was added and the mixture vigorously stirred for 24 h. Solvent was removed under reduced pressure, and the resulting solid was purified by column chromatography on silica gel ( $\text{AcOEt}$ :Hex 1:20), yielding **3a** as an orange solid (0.58 g, 85%).  $^1\text{H}$  NMR ( $\text{CDCl}_3$ , 400 MHz):  $\delta$  1.20 (s, 36H, 4  $\text{CMe}_3$ ), 1.38 (s, 36H, 4  $\text{CMe}_3$ ), 6.42 (d,  $^3J_{\text{HH}} = 8$  Hz, 2H, 2 H arom), 6.71 (t,  $^3J_{\text{HH}} = 7$  Hz, 6H, 6 H arom), 6.84 (t, 1H,  $^3J_{\text{HH}} = 8$  Hz, H arom), 6.97 (t,  $^3J_{\text{HH}} = 7$  Hz, 3H, 3 H arom), 7.10 (br s, 4H, 4 H arom), 7.33 (br s, 4H, 4 H arom), 7.35 (d,  $^3J_{\text{HH}} = 7$  Hz, 6H, 6 H arom).  $^{31}\text{P}\{^1\text{H}\}$  NMR ( $\text{CDCl}_3$ , 162.1 MHz):  $\delta$  28.6 (td,  $J_{\text{PRh}} = 129$  Hz,  $J_{\text{PP}} = 44$  Hz, P-C), 171.5 (dd,  $J_{\text{PRh}} = 265$  Hz, P-O).  $^{13}\text{C}\{^1\text{H}\}$  NMR ( $\text{CDCl}_3$ , 75.5 MHz):  $\delta$  31.8 (s, 4  $\text{CMe}_3$ ), 31.9 (s, 4  $\text{CMe}_3$ ), 35.0 (s, 4  $\text{CMe}_3$ ), 35.8 (s, 4  $\text{CMe}_3$ ), 105.3 (t,  $J_{\text{PC}} = 8$  Hz, 2 CH arom), 124.6 (s, 4 CH arom), 126.0 (s, CH arom), 127.6 (s, 4 CH arom), 128.0 (d,  $J_{\text{PC}} = 9$  Hz, 6 CH arom), 129.0 (s, 3 CH arom), 131.4 (s, 4  $\text{C}_q$  arom), 134.0 (d,  $J_{\text{PC}} = 13$  Hz, 6 CH arom), 137.7 (d,  $J_{\text{PC}} = 36$  Hz, 3  $\text{C}_q$  arom), 140.1 (s, 4  $\text{C}_q$  arom), 140.7 (ddd,  $J_{\text{PC}} = 58$ , 14 Hz,  $J_{\text{RhC}} = 28$  Hz,  $\text{C}_q$  arom), 146.6 (s, 4  $\text{C}_q$  arom), 147.4 (t,  $J_{\text{PC}} = 5$  Hz, 4  $\text{OC}_q$  arom), 159.5 (t,  $J_{\text{PC}} = 13$  Hz, 2  $\text{OC}_q$  arom). Anal. Calcd for  $\text{C}_{80}\text{H}_{98}\text{O}_6\text{P}_3\text{Rh}$ : C, 71.1; H, 7.3. Found: C, 70.6; H, 7.4.



**Rh(PCP<sup>b</sup>)(PPh<sub>3</sub>) (5b).** Over a suspension of RhCl(PPh<sub>3</sub>)<sub>3</sub> (0.473 g, 0.54 mmol) in THF (5 mL) was added diphosphite **2b** (0.500 g, 0.54 mmol) dissolved in THF (5 mL). The mixture was heated over 16 h at 60 °C. An excess of NEt<sub>3</sub> (0.1 mL) was added and the mixture vigorously stirred for 24 h at 60 °C. Solvent was removed under reduced pressure, and the resulting solid was purified by column chromatography on silica gel (AcOEt:hexane, 1:20), yielding **5b** as an orange solid (0.474 g, 71%). <sup>1</sup>H NMR (CD<sub>2</sub>Cl<sub>2</sub>, 500 MHz): δ 1.13 (s, 18H, 2 CMe<sub>3</sub>), 1.42 (s, 18H, 2 CMe<sub>3</sub>), 1.76 (s, 6H, 2 Ar-Me), 1.82 (s, 6H, 2 Ar-Me), 2.23 (s, 6H, 2 Ar-Me), 2.32 (s, 6H, 2 Ar-Me), 6.41 (d, <sup>3</sup>J<sub>HH</sub> = 7.5 Hz, 2H, 2 H arom), 6.62 (s, 2H, 2 H arom), 6.90 (m, 7H, 7 H arom), 7.10 (t, <sup>3</sup>J<sub>HH</sub> = 7.5 Hz, 3H, 3 H arom), 7.24 (s, 2H, 2 H arom), 7.42 (dd, <sup>3</sup>J<sub>HP</sub> = 9.0 Hz, <sup>3</sup>J<sub>HH</sub> = 9.0 Hz, 6H, 6 H arom). <sup>31</sup>P{<sup>1</sup>H} NMR (CD<sub>2</sub>Cl<sub>2</sub>, 202.4 MHz): δ 25.5 (dt, *J*<sub>PRh</sub> = 127 Hz, *J*<sub>PP</sub> = 43 Hz, P-C), 165.6 (dd, *J*<sub>PRh</sub> = 266 Hz, P-O). <sup>13</sup>C{<sup>1</sup>H} NMR (CD<sub>2</sub>Cl<sub>2</sub>, 125.8 MHz): δ 16.7 (s, 2 Ar-Me), 17.0 (s, 2 Ar-Me), 20.4 (s, 2 Ar-Me), 20.6 (s, 2 Ar-Me), 32.1 (s, 4 CMe<sub>3</sub>), 34.8 (s, 2 CMe<sub>3</sub>), 35.2 (s, 2 CMe<sub>3</sub>), 104.8 (dd, *J*<sub>CRh</sub> = 7 Hz, *J*<sub>CP</sub> = 7 Hz, 2 CH arom), 126.5 (s, CH arom), 127.6 (d, *J*<sub>CP</sub> = 9 Hz, 6 CH arom), 128.2 (s, 2 CH arom), 128.3 (s, 2 CH arom), 128.7 (s, 3 CH arom), 129.0 (s, 2 C<sub>q</sub>), 130.6 (s, 2 C<sub>q</sub>), 132.1 (s, 2 C<sub>q</sub>), 133.3 (s, 2 C<sub>q</sub>), 134.7 (d, *J*<sub>CP</sub> = 13 Hz, 6 CH arom), 134.8 (s, 2 C<sub>q</sub>), 135.3 (s, 2 C<sub>q</sub>), 136.8 (s, 2 C<sub>q</sub>), 138.4 (s, 2 C<sub>q</sub>), 138.5 (d, *J*<sub>CP</sub> = 31 Hz, 3 C<sub>q</sub>), 140.4 (ddt, *J*<sub>CP</sub> = 59, 14 Hz, *J*<sub>CRh</sub> = 27 Hz, C<sub>q</sub>), 146.5 (s, 2 C<sub>q</sub>), 146.7 (s, 2 C<sub>q</sub>), 159.4 (dd, *J*<sub>CRh</sub> = 13 Hz, *J*<sub>CP</sub> = 13 Hz, 2 C<sub>q</sub>). Anal. Calcd for C<sub>72</sub>H<sub>82</sub>O<sub>6</sub>P<sub>3</sub>Rh: C, 69.8; H, 6.7. Found: C, 70.0; H, 6.9.

**Rh(PCP<sup>c</sup>)(PPh<sub>3</sub>) (5c).** Over a solution of RhCl(PPh<sub>3</sub>)<sub>3</sub> (0.200 g, 0.22 mmol) and diphosphite **2c** (0.224 g, 0.22 mmol) in THF (10 mL) was added an excess of NEt<sub>3</sub> (0.3 mL). The mixture was heated over 24 h at 70 °C. Solvent was removed under reduced pressure, and the resulting solid was purified by column chromatography on silica gel (AcOEt:hexane, 1:20), yielding **5c** as a yellow-orange solid (0.150 g, 49%). <sup>1</sup>H NMR (CDCl<sub>3</sub>, 400 MHz): δ 1.15 (s, 18H, 2 CMe<sub>3</sub>), 1.25 (s, 18H, 2 CMe<sub>3</sub>), 1.42 (s, 18H, 2 CMe<sub>3</sub>), 1.43 (s, 18H, 2 CMe<sub>3</sub>), 6.76 (t, <sup>3</sup>J<sub>HH</sub> = 7.6 Hz, 6H, 6 H arom), 6.87 (s, 1H, H arom), 7.03 (m, 4H, 4 H arom), 7.14 (m, 2H, 2 H arom), 7.21 (m, 3H, 3 H arom), 7.32 (d, <sup>3</sup>J<sub>HH</sub> = 8.4 Hz, 1H, H arom), 7.37 (m, 4H, 4 H arom), 7.43 (m, 6H, 6 H arom), 7.56 (d, <sup>3</sup>J<sub>HH</sub> = 8.0 Hz, 1H, H arom). <sup>31</sup>P{<sup>1</sup>H} NMR (CDCl<sub>3</sub>, 162.1 MHz): δ 28.7 (dt, *J*<sub>PRh</sub> = 128 Hz, *J*<sub>PP</sub> = 44 Hz, P-C), 168.1 (ddd, *J*<sub>PP</sub> = 694 Hz, *J*<sub>PRh</sub> = 265 Hz, *J*<sub>PP</sub> = 44 Hz, P-O), 173.1 (ddd, *J*<sub>PP</sub> = 694 Hz, *J*<sub>PRh</sub> = 265 Hz, *J*<sub>PP</sub> = 44 Hz, P-O). <sup>13</sup>C{<sup>1</sup>H} NMR (CDCl<sub>3</sub>, 125.8 MHz): δ 31.2 (s, 2 CMe<sub>3</sub>), 31.5 (s, 2 CMe<sub>3</sub>), 31.6 (s, 4 CMe<sub>3</sub>), 34.7 (s, 2 CMe<sub>3</sub>), 34.7 (s, 2 CMe<sub>3</sub>), 35.5 (s, 2 CMe<sub>3</sub>), 35.6 (s, 2 CMe<sub>3</sub>), 110.1 (d, *J*<sub>CP</sub> = 13 Hz, CH arom), 118.1 (d, *J*<sub>CP</sub> = 13 Hz, C<sub>q</sub>), 122.3 (s, CH arom), 122.7 (s, CH arom), 124.3 (s, 2 CH arom), 124.4 (s, 3 CH arom), 126.6 (s, CH arom), 127.3 (s, 2 CH arom), 127.4 (s, 2 CH arom), 127.8 (d, *J*<sub>CP</sub> = 9 Hz, 6 CH arom), 128.5 (m, C<sub>q</sub>), 128.7 (s, 3 CH arom), 131.0 (s, 2 C<sub>q</sub>), 131.2 (s, 2 C<sub>q</sub>), 133.8 (d, *J*<sub>CP</sub> = 13 Hz, 6 CH arom), 133.9 (s, 2 C<sub>q</sub>), 137.4 (d, *J*<sub>CP</sub> = 36 Hz, 3 C<sub>q</sub>), 139.8 (d, *J*<sub>CP</sub> = 5 Hz, 2 C<sub>q</sub>), 139.9 (ddt, *J*<sub>CP</sub> = 59, 14 Hz, *J*<sub>CRh</sub> = 28 Hz, C<sub>q</sub>), 146.4 (s, 4 C<sub>q</sub>), 147.1 (d, *J*<sub>CP</sub> = 10 Hz, 2 C<sub>q</sub>), 147.3 (d, *J*<sub>CP</sub> = 10 Hz, 2 C<sub>q</sub>), 153.9 (d, *J*<sub>CP</sub> = 20 Hz, C<sub>q</sub>), 157.7 (d, *J*<sub>CP</sub> = 19 Hz, C<sub>q</sub>). Anal. Calcd for C<sub>84</sub>H<sub>100</sub>O<sub>6</sub>P<sub>3</sub>Rh: C, 72.0; H, 7.2. Found: C, 72.1; H, 7.3.

**Rh(PCP<sup>a</sup>)(CO) (6a).** To a solution of compound **3a** (0.04 g, 0.03 mmol) in THF (10 mL) was added an excess of elemental selenium (0.005 g, 0.06 mmol). The mixture was introduced in a Fischer–Porter vessel and charged with 2 atm of CO. After 1 h the reactor was vented and solvent removed. The solution was concentrated until turbidity and filtered. After the mixture stood for 24 h, compound **4a** was collected as yellow crystals (0.020 g, 60%). IR (Nujol mull, cm<sup>-1</sup>): 2017 (ν<sub>CO</sub>). <sup>1</sup>H NMR (CDCl<sub>3</sub>, 500 MHz): δ 1.33 (s, 36H, 4 CMe<sub>3</sub>), 1.40 (s, 36H, 4 CMe<sub>3</sub>), 6.64 (d, <sup>3</sup>J<sub>HH</sub> = 8 Hz, 2H, 2 H arom), 7.05 (t, <sup>3</sup>J<sub>HH</sub> = 8 Hz, 1H, H arom), 7.20 (d, <sup>4</sup>J<sub>HH</sub> = 2 Hz, 4H, 4 H arom), 7.45 (d, <sup>4</sup>J<sub>HH</sub> = 2 Hz, 4H, 4 H arom). <sup>31</sup>P{<sup>1</sup>H}

NMR (CDCl<sub>3</sub>, 162.1 MHz): δ 167.3 (d, *J*<sub>PRh</sub> = 256 Hz). <sup>13</sup>C{<sup>1</sup>H} NMR (CDCl<sub>3</sub>, 125.8 MHz): δ 31.5 (s, 4 CMe<sub>3</sub>), 31.7 (s, 4 CMe<sub>3</sub>), 34.7 (4 CMe<sub>3</sub>), 35.7 (4 CMe<sub>3</sub>), 106.1 (t, *J*<sub>PC</sub> = 8 Hz, 2 CH arom), 125.0 (s, 4 CH arom), 126.6 (s, 4 CH arom), 129.5 (s, CH arom), 131.6 (s, 4 C<sub>q</sub> arom), 140.2 (m, C<sub>q</sub> arom), 140.3 (s, 4 C<sub>q</sub> arom), 145.1 (s, 4 OC<sub>q</sub> arom), 147.6 (s, 4 C<sub>q</sub> arom), 160.4 (t, *J*<sub>PC</sub> = 14 Hz, 2 OC<sub>q</sub> arom), 191.8 (dt, *J*<sub>RhC</sub> = 58 Hz, *J*<sub>PC</sub> = 16 Hz, CO). Anal. Calcd for C<sub>63</sub>H<sub>83</sub>O<sub>7</sub>P<sub>2</sub>Rh: C, 67.7; H, 7.5. Found: C, 67.9; H, 7.9.

**Rh(PCP<sup>a</sup>)(CNXy) (7a).** A mixture of **5a** (0.04 g, 0.03 mmol), elemental Se (4 mg, 0.05 mmol), and CNXy (0.004 g, 0.03 mmol) in THF was vigorously stirred for 30 min. Solvent was removed under reduced pressure, and the obtained residue was extracted with *n*-pentane (3 × 10 mL). The solution was concentrated until turbidity appeared and then filtered. The resulting solution was left to stand for 24 h, and then compound **7a** appeared as yellow crystals (0.035 g, 95%). IR (Nujol mull, cm<sup>-1</sup>): 2099 (s, ν<sub>CN</sub>). <sup>1</sup>H NMR (CDCl<sub>3</sub>, 500 MHz): δ 1.31 (s, 36H, 4 CMe<sub>3</sub>), 1.40 (br s, 36H, 4 CMe<sub>3</sub>), 1.55 (s, 6H, 2 Me), 6.59 (d, <sup>3</sup>J<sub>HH</sub> = 7.5 Hz, 2H, 2 H arom), 6.75 (d, <sup>3</sup>J<sub>HH</sub> = 7.5 Hz, 2H, 2 H arom), 6.92 (t, <sup>3</sup>J<sub>HH</sub> = 7.5 Hz, 1H, H arom), 6.95 (t, <sup>3</sup>J<sub>HH</sub> = 7.5 Hz, 1H, H arom), 7.18 (d, <sup>4</sup>J<sub>HH</sub> = 2.5 Hz, 4H, 4 H arom), 7.40 (d, <sup>4</sup>J<sub>HH</sub> = 2.5 Hz, 4H, 4 H arom). <sup>31</sup>P{<sup>1</sup>H} NMR (CDCl<sub>3</sub>, 162.1 MHz): δ 170.1 (d, *J*<sub>PRh</sub> = 265 Hz). <sup>13</sup>C{<sup>1</sup>H} NMR (CDCl<sub>3</sub>, 125.8 MHz): δ 18.2 (s, 2 Ar-Me), 31.5 (s, 4 CMe<sub>3</sub>), 31.8 (s, 4 CMe<sub>3</sub>), 34.7 (s, 4 CMe<sub>3</sub>), 35.7 (s, 4 CMe<sub>3</sub>), 105.6 (t, 2 CH arom), 124.7 (s, 4 CH arom), 126.5 (s, 4 CH arom), 127.1 (s, CH arom), 127.2 (s, 2 CH arom), 131.6 (s, 2 C<sub>q</sub> arom), 132.0 (s, 4 C<sub>q</sub> arom), 134.7 (s, CH arom), 140.6 (s, 4 C<sub>q</sub> arom), 142.1 (dt, *J*<sub>RhC</sub> = 25 Hz, *J*<sub>PC</sub> = 15 Hz), 143.8 (s, C<sub>q</sub> arom), 145.3 (s, 4 OC<sub>q</sub> arom), 146.9 (s, 4 C<sub>q</sub> arom), 160.4 (t, *J*<sub>PC</sub> = 15 Hz, 2 OC<sub>q</sub> arom), 163.0 (dt, *J*<sub>RhC</sub> = 56 Hz, *J*<sub>PC</sub> = 18 Hz, CN). Anal. Calcd for C<sub>71</sub>H<sub>92</sub>NO<sub>6</sub>P<sub>2</sub>Rh·0.5CH<sub>2</sub>Cl<sub>2</sub>: C, 68.0; H, 7.4; N, 1.1. Found: C, 68.4; H, 7.4; N, 1.2.

**Rh(PCP<sup>a</sup>)(η<sup>2</sup>-C<sub>2</sub>H<sub>4</sub>) (8a).** In a Fischer–Porter vessel compound **3a** (0.108 g, 0.08 mmol) and Se (0.010 g, 0.13 mmol) were added to THF (10 mL). The reactor was charged with 4 atm of C<sub>2</sub>H<sub>4</sub> and heated at 40 °C. Reaction completion was observed after 4 days. Solvent was removed under reduced pressure and the remaining solid extracted with *n*-pentane (3 × 10 mL). Further filtration and concentration yielded **5a** as orange crystals (0.040 g, 45%). <sup>1</sup>H NMR (CD<sub>2</sub>Cl<sub>2</sub>, 400 MHz): δ 1.30 (s, 36H, 4 CMe<sub>3</sub>), 1.39 (s, 36H, 4 CMe<sub>3</sub>), 2.82 (br s, 4H, C<sub>2</sub>H<sub>4</sub>), 6.68 (d, <sup>3</sup>J<sub>HH</sub> = 8 Hz, 2H, 2 H arom), 7.01 (t, <sup>3</sup>J<sub>HH</sub> = 8 Hz, 1H, H arom), 7.28 (d, <sup>4</sup>J<sub>HH</sub> = 2.5 Hz, 4H, 4 H arom), 7.50 (d, <sup>4</sup>J<sub>HH</sub> = 2.5 Hz, 4H, 4 H arom). <sup>31</sup>P{<sup>1</sup>H} NMR (CD<sub>2</sub>Cl<sub>2</sub>, 162.1 MHz): δ 177.3 (d, *J*<sub>PRh</sub> = 253 Hz). <sup>13</sup>C{<sup>1</sup>H} NMR (CDCl<sub>3</sub>, 75.5 MHz): δ 31.5 (s, 4 CMe<sub>3</sub>), 31.5 (s, 4 CMe<sub>3</sub>), 34.7 (s, 4 CMe<sub>3</sub>), 35.6 (s, 4 CMe<sub>3</sub>), 58.8 (br s, C<sub>2</sub>H<sub>4</sub>), 105.7 (t, *J*<sub>PC</sub> = 9 Hz, 2 CH arom), 124.8 (s, 4 CH arom), 125.2 (s, CH arom), 126.7 (s, 4 CH arom), 131.6 (s, 4 C<sub>q</sub> arom), 139.9 (dt, *J*<sub>RhC</sub> = 29 Hz, *J*<sub>PC</sub> = 16 Hz, C<sub>q</sub> arom), 140.1 (s, 4 C<sub>q</sub> arom), 145.5 (br s, 4 OC<sub>q</sub> arom), 147.4 (s, 4 C<sub>q</sub> arom), 158.8 (t, *J*<sub>PC</sub> = 16 Hz, 2 OC<sub>q</sub> arom). Anal. Calcd for C<sub>64</sub>H<sub>87</sub>O<sub>6</sub>P<sub>2</sub>Rh: C, 68.8; H, 7.8. Found: C, 69.0; H, 8.2.

**Rh(PCP<sup>b</sup>)(η<sup>2</sup>-C<sub>2</sub>H<sub>4</sub>) (8b).** In a Fischer–Porter vessel compound **5b** (0.100 g, 0.08 mmol) and Se (0.007 g, 0.09 mmol) were added to THF (5 mL). The reactor was charged with 4 atm of C<sub>2</sub>H<sub>4</sub> and heated at 65 °C for 5 days. Solvent was removed under reduced pressure and the remaining solid purified by chromatography on a silica gel column (CH<sub>2</sub>Cl<sub>2</sub>:hexane, 1:10). Compound **8b** was obtained as a yellow solid (0.045 g, 56%). <sup>1</sup>H NMR (CD<sub>2</sub>Cl<sub>2</sub>, 400 MHz): δ 1.19 (s, 18H, 2 CMe<sub>3</sub>), 1.37 (s, 18H, 2 CMe<sub>3</sub>), 1.88 (s, 6H, 2 Ar-Me), 1.96 (s, 6H, 2 Ar-Me), 2.28 (d, *J*<sub>app</sub> = 10 Hz, 2H, C<sub>2</sub>H<sub>4</sub>), 2.33 (s, 6H, 2 Ar-Me), 2.36 (s, 6H, 2 Ar-Me), 2.98 (d, *J*<sub>app</sub> = 10 Hz, 2H, C<sub>2</sub>H<sub>4</sub>), 6.64 (d, <sup>3</sup>J<sub>HH</sub> = 8.0 Hz, 2H, 2 H arom), 6.97 (t, <sup>3</sup>J<sub>HH</sub> = 8.0 Hz, 1H, H arom), 7.18 (s, 2H, 2 H arom), 7.33 (s, 2H, 2 H arom). <sup>31</sup>P{<sup>1</sup>H} NMR (CD<sub>2</sub>Cl<sub>2</sub>, 162.1 MHz): δ 175.1 (d, *J*<sub>PRh</sub> = 253 Hz). <sup>13</sup>C{<sup>1</sup>H} NMR (CD<sub>2</sub>Cl<sub>2</sub>, 75.5 MHz): δ 16.7 (s, 2 Ar-Me), 16.8 (s, 2 Ar-Me), 20.5 (s, 2 Ar-Me), 20.6 (s, 2 Ar-Me),

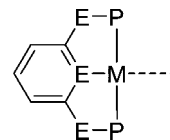
31.8 (s, 2 CMe<sub>3</sub>), 32.0 (s, 2 CMe<sub>3</sub>), 35.2 (s, 4 CMe<sub>3</sub>), 58.6 (br d,  $J_{CP}$  = 4 Hz, C<sub>2</sub>H<sub>4</sub>), 105.9 (dd,  $J_{CRh}$  = 9 Hz,  $J_{CP}$  = 9 Hz, 2 CH arom), 125.5 (s, CH arom), 128.9 (s, 2 CH arom), 129.2 (s, 2 CH arom), 130.4 (s, 2 C<sub>q</sub>), 130.7 (s, 2 C<sub>q</sub>), 133.6 (s, 2 C<sub>q</sub>), 133.6 (s, 2 C<sub>q</sub>), 135.4 (s, 2 C<sub>q</sub>), 135.8 (s, 2 C<sub>q</sub>), 137.9 (s, 2 C<sub>q</sub>), 138.0 (s, 2 C<sub>q</sub>), 140.0 (dt,  $J_{CRh}$  = 29 Hz,  $J_{CP}$  = 16 Hz, C<sub>q</sub>), 145.3 (dd,  $J_{CRh}$  = 5 Hz,  $J_{CP}$  = 5 Hz, 2 C<sub>q</sub>), 145.6 (s, 2 C<sub>q</sub>), 159.4 (dd,  $J_{CRh}$  = 16 Hz,  $J_{CP}$  = 16 Hz, 2 C<sub>q</sub>). Anal. Calcd for C<sub>56</sub>H<sub>71</sub>O<sub>6</sub>P<sub>2</sub>Rh: C, 66.9; H, 7.1. Found: C, 66.5; H, 7.3.

**Rh(PCP<sup>c</sup>)( $\eta^2$ -C<sub>2</sub>H<sub>4</sub>) (8c).** In a Fischer–Porter vessel compound **5c** (0.200 g, 0.14 mmol) and Se (0.014 g, 0.18 mmol) were added to THF (5 mL). The reactor was charged with 4 atm of C<sub>2</sub>H<sub>4</sub> and heated at 50 °C for 3 days. Solvent was removed under reduced pressure and the remaining solid extracted with *n*-pentane (3 × 10 mL) and purified by chromatography on a silica gel column (hexane). Compound **8c** was obtained as a yellow solid (0.075 g, 46%). <sup>1</sup>H NMR (CD<sub>2</sub>Cl<sub>2</sub>, 500 MHz):  $\delta$  1.27 (s, 36H, 4 CMe<sub>3</sub>), 1.35 (s, 18H, 2 CMe<sub>3</sub>), 1.36 (s, 18H, 2 CMe<sub>3</sub>), 2.80 (br s, 4H, C<sub>2</sub>H<sub>4</sub>), 7.08 (s, 1H, H arom), 7.21 (m, 1H, H arom), 7.28 (m, 5H, 5 H arom), 7.48 (s, 4H, 4 H arom), 7.65 (d,  $^3J_{HH}$  = 8.0 Hz, 1H, H arom), 7.83 (d,  $^3J_{HH}$  = 7.6 Hz, 1H, H arom). <sup>31</sup>P{<sup>1</sup>H} NMR (CD<sub>2</sub>Cl<sub>2</sub>, 202.4 MHz):  $\delta$  174.6 (dd,  $J_{PP}$  = 590 Hz,  $J_{PRh}$  = 253 Hz, P–O), 178.0 (dd,  $J_{PP}$  = 590 Hz,  $J_{PRh}$  = 252 Hz, P–O). <sup>13</sup>C{<sup>1</sup>H} NMR (CD<sub>2</sub>Cl<sub>2</sub>, 125.8 MHz):  $\delta$  31.5 (s, 2 CMe<sub>3</sub>), 31.6 (s, 6 CMe<sub>3</sub>), 35.0 (s, 4 CMe<sub>3</sub>), 35.8 (s, 2 CMe<sub>3</sub>), 35.9 (s, 2 CMe<sub>3</sub>), 59.5 (br s, C<sub>2</sub>H<sub>4</sub>), 101.6 (d,  $J_{CP}$  = 13 Hz, CH arom), 118.8 (d,  $J_{CP}$  = 12 Hz, C<sub>q</sub>), 122.3 (s, CH arom), 124.0 (s, CH arom), 125.0 (s, CH arom), 125.4 (s, 4 CH arom), 127.1 (s, 2 CH arom), 127.1 (s, 2 CH arom), 127.3 (s, CH arom), 131.9 (s, 2 C<sub>q</sub>), 131.9 (s, 2 C<sub>q</sub>), 133.7 (s, C<sub>q</sub>), 139.5 (m, C<sub>q</sub>), 140.5 (s, 2 C<sub>q</sub>), 140.6 (s, 2 C<sub>q</sub>), 145.9 (m, 4 C<sub>q</sub>), 148.2 (s, 4 C<sub>q</sub>), 153.6 (dd,  $J_{CP}$  = 23 Hz,  $J_{CRh}$  = 9 Hz, C<sub>q</sub>), 157.6 (dd,  $J_{CP}$  = 23 Hz,  $J_{CRh}$  = 9 Hz, C<sub>q</sub>). Anal. Calcd for C<sub>68</sub>H<sub>89</sub>O<sub>6</sub>P<sub>2</sub>Rh: C, 70.0; H, 7.7. Found: C, 69.7; H, 7.9.

**Rh(PCP<sup>a</sup>)( $\eta^2$ -MeC<sub>2</sub>H<sub>3</sub>) (9a).** In a Fischer–Porter vessel compound **8a** (0.100 g, 0.09 mmol) was added to THF (5 mL). The reactor was charged with 1 atm of propene at room temperature and stirred for 5 days, with the propene atmosphere replaced every 24 h. Solvent was removed under reduced pressure, yielding compound **9a**, accompanied by a minor amount of **8a** (< 3%), as a yellow solid (0.100 g, quantitative). All attempts to further purify compound **9a** were unsuccessful. <sup>1</sup>H NMR (CD<sub>2</sub>Cl<sub>2</sub>, 300 MHz):  $\delta$  1.06 (d,  $^3J_{HH}$  = 5.4 Hz, 3H, MeCH=CH<sub>2</sub>), 1.31 (s, 18H, 2 CMe<sub>3</sub>), 1.38 (s, 18H, 2 CMe<sub>3</sub>), 1.39 (s, 18H, 2 CMe<sub>3</sub>), 1.41 (s, 18H, 2 CMe<sub>3</sub>), 2.51 (br d,  $^3J_{HH}$  = 8.7 Hz, 1H, MeCH=CH<sub>2</sub>), 3.29 (br d,  $^3J_{HH}$  = 12.3 Hz, 1H, MeCH=CH<sub>2</sub>), 4.39 (br m, 1H, MeCH=CH<sub>2</sub>), 6.66 (d,  $^3J_{HH}$  = 7.8 Hz, 2H, 2 H arom), 7.00 (t,  $^3J_{HH}$  = 8.1 Hz, 1H, H arom), 7.25 (d,  $^4J_{HH}$  = 2.4 Hz, 2H, 2 H arom), 7.32 (d,  $^4J_{HH}$  = 2.4 Hz, 2H, 2 H arom), 7.48 (d,  $^4J_{HH}$  = 2.1 Hz, 2H, 2 H arom), 7.55 (d,  $^4J_{HH}$  = 2.4 Hz, 2H, 2 H arom). <sup>31</sup>P{<sup>1</sup>H} NMR (CD<sub>2</sub>Cl<sub>2</sub>, 121.5 MHz):  $\delta$  171.6 (d,  $J_{PRh}$  = 259 Hz). <sup>13</sup>C{<sup>1</sup>H} NMR (CD<sub>2</sub>Cl<sub>2</sub>, 75.5 MHz):  $\delta$  19.5 (s, MeCH=CH<sub>2</sub>), 31.5 (s, 2 CMe<sub>3</sub>), 31.7 (s, 4 CMe<sub>3</sub>), 32.0 (s, 2 CMe<sub>3</sub>), 35.1 (s, 4 CMe<sub>3</sub>), 35.9 (s, 4 CMe<sub>3</sub>), 65.0 (s, MeCH=CH<sub>2</sub>), 78.2 (s, MeCH=CH<sub>2</sub>), 106.0 (dd,  $J_{CRh}$  = 9 Hz,  $J_{CP}$  = 9 Hz, 2 CH arom), 125.2 (s, 2 CH arom), 125.3 (s, 2 CH arom), 125.8 (s, CH arom), 126.9 (s, 2 CH arom), 127.2 (s, 2 CH arom), 131.7 (s, 2 C<sub>q</sub>), 132.2 (s, 2 C<sub>q</sub>), 139.3 (dt,  $J_{CRh}$  = 30 Hz,  $J_{CP}$  = 17 Hz, C<sub>q</sub>), 140.6 (s, 4 C<sub>q</sub>), 145.6 (s, 2 C<sub>q</sub>), 146.1 (s, 2 C<sub>q</sub>), 147.9 (s, 2 C<sub>q</sub>), 148.3 (s, 2 C<sub>q</sub>), 159.3 (dd,  $J_{CRh}$  = 15 Hz,  $J_{CP}$  = 15 Hz, 2 C<sub>q</sub>).

**Rh(PCP<sup>b</sup>)( $\eta^2$ -MeC<sub>2</sub>H<sub>3</sub>) (9b).** In a Fischer–Porter vessel compound **8b** (0.020 g, 0.02 mmol) was added to THF (3 mL), and the reactor was charged with 1 atm of propene and stirred for 9 days, with the propene atmosphere renewed every 24 h. Solvent was removed under reduced pressure. Compound **9b** was obtained as a yellow solid, contaminated with minor amounts of **8b** (< 5%) (0.020 g, quantitative). All attempts to further purify compound **9b** were unsuccessful. <sup>1</sup>H NMR (CD<sub>2</sub>Cl<sub>2</sub>, 500 MHz):  $\delta$  1.03 (d,

Chart 1



$^3J_{HH}$  = 4.0 Hz, 3H, MeCH=CH<sub>2</sub>), 1.22 (s, 18H, 2 CMe<sub>3</sub>), 1.35 (s, 18H, 2 CMe<sub>3</sub>), 1.84 (s, 6H, 2 Ar-Me), 1.94 (s, 6H, 2 Ar-Me), 2.33 (s, 6H, 2 Ar-Me), 2.37 (s, 6H, 2 Ar-Me), 2.38 (br d,  $^3J_{HH}$  = 9.0 Hz, 1H, MeCH=CH<sub>2</sub>), 3.83 (br d,  $^3J_{HH}$  = 13.5 Hz, 1H, MeCH=CH<sub>2</sub>), 3.86 (br m, 1H, MeCH=CH<sub>2</sub>), 6.58 (d,  $^3J_{HH}$  = 8.0 Hz, 2H, 2 H arom), 6.93 (t,  $^3J_{HH}$  = 8.0 Hz, 1H, H arom), 7.17 (s, 2H, 2 H arom), 7.29 (s, 2H, 2 H arom). <sup>31</sup>P{<sup>1</sup>H} NMR (CD<sub>2</sub>Cl<sub>2</sub>, 202.4 MHz):  $\delta$  169.5 (d,  $J_{PRh}$  = 258 Hz). <sup>13</sup>C{<sup>1</sup>H} NMR (CD<sub>2</sub>Cl<sub>2</sub>, 125.8 MHz):  $\delta$  16.6 (s, 2 Ar-Me), 16.6 (s, 2 Ar-Me), 18.9 (s, MeCH=CH<sub>2</sub>), 20.4 (s, 2 Ar-Me), 20.6 (s, 2 Ar-Me), 31.7 (s, 2 CMe<sub>3</sub>), 32.0 (s, 2 CMe<sub>3</sub>), 35.1 (s, 2 CMe<sub>3</sub>), 35.2 (s, 2 CMe<sub>3</sub>), 64.5 (s, MeCH=CH<sub>2</sub>), 76.9 (s, MeCH=CH<sub>2</sub>), 105.8 (dd,  $J_{CRh}$  = 9 Hz,  $J_{CP}$  = 9 Hz, 2 CH arom), 125.2 (s, CH arom), 128.6 (s, 2 CH arom), 129.0 (s, 2 CH arom), 130.4 (s, 2 C<sub>q</sub>), 130.9 (s, 2 C<sub>q</sub>), 133.4 (s, 2 C<sub>q</sub>), 133.5 (s, 2 C<sub>q</sub>), 135.3 (s, 2 C<sub>q</sub>), 135.7 (s, 2 C<sub>q</sub>), 137.9 (s, 2 C<sub>q</sub>), 138.3 (s, 2 C<sub>q</sub>), 139.5 (m, C<sub>q</sub>), 145.5 (dd,  $J_{CRh}$  = 5 Hz,  $J_{CP}$  = 5 Hz, 2 C<sub>q</sub>), 145.6 (s, 2 C<sub>q</sub>), 159.2 (dd,  $J_{CRh}$  = 16 Hz,  $J_{CP}$  = 16 Hz, 2 C<sub>q</sub>).

**QUEST3D Search Details.** The QUEST3D searches commented in the text have been carried out on the Cambridge Structural Database (updated Nov 2007) and have the following details. (a) For the analysis of the P–M–P angles in square-planar transition-metal complexes containing a pincer ligand (see see Chart 1, E is any atom), the CSD search with restrictions (not disordered, no errors,  $R \leq 0.075$ ) gave a mean value of 164° (89 fragments, 71 hits). (b) For the analysis of the C–C distance of ethylene rhodium complexes, the CSD search without any restriction gave a mean value of 1.39 Å (146 fragments, 70 hits). A similar value (1.38 Å for 121 fragments, 57 hits) was obtained with restrictions (not disordered, no errors,  $R \leq 0.075$ ). In this case the Rh–C mean value is 2.13 Å.

**Computational Details.** The electronic structures and geometries of the model complexes **I–VII** were computed within the density functional theory at the B3LYP level.<sup>33</sup> The Rh atom was described with the Stuttgart Relativistic Small Core ECP basis set<sup>34</sup> and a polarization function. In all cases the atoms corresponding to the pincer ligand are described using a TZVP basis set. For the more complex models **IV–VII**, the biphenyl groups are described using a DZVP basis set. All the calculations were performed using the Gaussian03 package.<sup>35</sup> Figures were drawn using Molekel.<sup>36</sup> XYZ coordinates of all optimized complexes are available upon request.

(33) (a) Becke, A. D. *J. Chem. Phys.* **1993**, *98*, 5648. (b) Lee, C. T.; Yang, W. T.; Parr, R. G. *Phys. Rev. B* **1988**, *37*, 785.

(34) Dolg, M.; Stoll, H.; Preuss, H.; Pitzer, R. M. *J. Phys. Chem.* **1993**, *97*, 5852.

(35) Frisch, M. J.; Trucks, G. W.; Schlegel, H. B.; Scuseria, G. E.; Robb, M. A.; Cheeseman, J. R.; Montgomery, Jr., J. A.; Vreven, T.; Kudin, K. N.; Burant, J. C.; Millam, J. M.; Iyengar, S. S.; Tomasi, J.; Barone, V.; Mennucci, B.; Cossi, M.; Scalmani, G.; Rega, N.; Petersson, G. A.; Nakatsuji, H.; Hada, M.; Ehara, M.; Toyota, K.; Fukuda, R.; Hasegawa, J.; Ishida, M.; Nakajima, T.; Honda, Y.; Kitao, O.; Nakai, H.; Klene, M.; Li, X.; Knox, J. E.; Hratchian, H. P.; Cross, J. B.; Bakken, V.; Adamo, C.; Jaramillo, J.; Gomperts, R.; Stratmann, R. E.; Yazyev, O.; Austin, A. J.; Cammi, R.; Pomelli, C.; Ochterski, J. W.; Ayala, P. Y.; Morokuma, K.; Voth, G. A.; Salvador, P.; Dannenberg, J. J.; Zakrzewski, V. G.; Dapprich, S.; Daniels, A. D.; Strain, M. C.; Farkas, O.; Malick, D. K.; Rabuck, A. D.; Raghavachari, K.; Foresman, J. B.; Ortiz, J. V.; Cui, Q.; Baboul, A. G.; Clifford, S.; Cioslowski, J.; Stefanov, B. B.; Liu, G.; Liashenko, A.; Piskorz, P.; Komaromi, I.; Martin, R. L.; Fox, D. J.; Keith, T.; Al-Laham, M. A.; Peng, C. Y.; Nanayakkara, A.; Challacombe, M.; Gill, P. M. W.; Johnson, B.; Chen, W.; Wong, M. W.; Gonzalez, C.; Pople, J. A. *Gaussian 03*, Revision C.02; Gaussian, Inc., Wallingford, CT, 2004.

(36) Portmann, S.; Luthi, H. P. *Chimia* **2000**, *54*, 766.

**X-ray Structure Determinations.** Crystallographic data were collected on a Bruker-Nonius X8Apex-II CCD diffractometer at 100(2) K using graphite-monochromated Mo K $\alpha_1$  radiation ( $\lambda = 0.710\,73\text{ \AA}$ ). The data were reduced (SAINT)<sup>37</sup> and corrected for Lorentz–polarization and absorption effects by a multiscan method (SADABS).<sup>38</sup> Structures were solved by direct methods (SIR-2002)<sup>39</sup> and refined against all  $F^2$  data by full-matrix least-squares techniques (SHELXTL-6.12).<sup>40</sup> All the non-hydrogen atoms were refined with anisotropic displacement parameters. The hydrogen atoms were included from calculated positions and refined riding on their respective carbon atoms with isotropic displacement parameters. A summary of cell parameters and data collection, structure solution, and refinement details is given in Table 6.

**Solid-State NMR.** Single-pulse MAS NMR spectra were recorded on a Bruker DRX400 spectrometer with a magnetic field of 9.36 T and equipped with a multinuclear probe. Powdered samples were packed in 4 mm zirconia rotors and spun at 10 KHz. <sup>31</sup>P MAS

NMR spectra were acquired at a frequency of 161.98 MHz, using a  $\pi/4$  pulse width of 3.58  $\mu\text{s}$  and a pulse space of 0.1 s. The <sup>13</sup>C MAS NMR spectrum was recorded at 104.26 MHz with proton decoupling, a pulse width of 2.5  $\mu\text{s}$  ( $\pi/2$  pulse length 7.5  $\mu\text{s}$ ), and a delay time of 2 s. The chemical shifts are reported in ppm from tetramethylsilane for <sup>1</sup>H and <sup>13</sup>C and from 87% solutions of H<sub>3</sub>PO<sub>4</sub> for <sup>31</sup>P.

**Acknowledgment.** We gratefully acknowledge Dr. M. D. Alba (ICMSE) for acquiring solid-state NMR spectra. The Ministerio de Educación y Ciencia (CTQ2006-05527, FED-ER support, and CONSOLIDER-INGENIO, CSD2007-00006) and Junta de Andalucía are also thanked for financial support. M.R. thanks the Ministerio de Educación y Ciencia for a FPU fellowship and D.d.R. the 6th FP of the EU for a MC-OIF.

**Supporting Information Available:** Figures giving selected NMR spectra and graphics for olefin rotation barriers and CIF files giving crystallographic details. This material is available free of charge via the Internet at <http://pubs.acs.org>.

OM800830W

(37) SAINT 6.02; Bruker-AXS, Inc., Madison, WI 53711-5373, 1997–1999.

(38) Sheldrick, G. SADABS; Bruker AXS, Inc., Madison, WI, 1999.

(39) Burla, M. C.; Camalli, M.; Carrozzini, B.; Cascarano, G. L.; Giacovazzo, C.; Polidori, G.; Spagna, R. *J. Appl. Crystallogr.* **2003**, *36*, 1103.

(40) SHELXTL 6.14; Bruker AXS, Inc. Madison, WI, 2000–2003.